

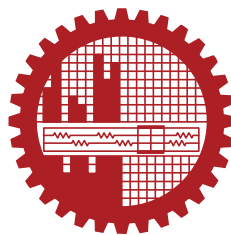
ESTIMATION AND ENHANCEMENT OF LIGHT EXTRACTION EFFICIENCY OF III-NITRIDE NANOWIRE BASED LIGHT EMITTING DIODES

by

Tashfiq Ahmed

0421062314

MASTER OF SCIENCE
IN
ELECTRICAL AND ELECTRONIC ENGINEERING



Department of Electrical and Electronic Engineering
Bangladesh University of Engineering and Technology

Dhaka, Bangladesh

July, 2023

The thesis titled, “**ESTIMATION AND ENHANCEMENT OF LIGHT EXTRACTION EFFICIENCY OF III-NITRIDE NANOWIRE BASED LIGHT EMITTING DIODES**”, submitted by **Tashfiq Ahmed**, Roll No.: 0421062314, Session: April 2021, has been accepted as satisfactory in partial fulfillment of the requirements for the degree of Master of Science in Electrical and Electronic Engineering on 23rd July, 2023.

BOARD OF EXAMINERS



Dr. Md Zunaid Baten
Associate Professor
Dept. of EEE, BUET, Dhaka

Chairman
(Supervisor)



Dr. Md. Aynal Haque
Professor and Head
Dept. of EEE, BUET, Dhaka

Member
(Ex-Officio)



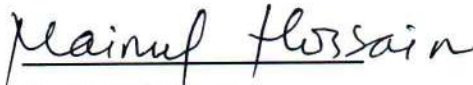
Dr. Sharif Mohammad Mominuzzaman
Professor
Dept. of EEE, BUET, Dhaka

Member



Dr. Sajid Muhaimin Choudhury
Assistant Professor
Dept. of EEE, BUET, Dhaka

Member



Dr. Mainul Hossain
Assistant Professor
Dept. of EEE, University of Dhaka, Dhaka

Member
(External)

Candidate's Declaration

This is to certify that the work presented in this thesis entitled, "ESTIMATION AND ENHANCEMENT OF LIGHT EXTRACTION EFFICIENCY OF III-NITRIDE NANOWIRE BASED LIGHT EMITTING DIODES", is the outcome of the research carried out by Tashfiq Ahmed under the supervision of Dr. Md Zunaid Baten, Associate Professor, Department of Electrical and Electronic Engineering, Bangladesh University of Engineering and Technology (BUET), Dhaka-1205, Bangladesh.

It is also declared that neither this thesis nor any part thereof has been submitted anywhere else for the award of any degree, diploma, or other qualifications.

Signature of the Candidate



Tashfiq Ahmed
0421062314

Dedication

I dedicate my thesis to my family and friends, especially my mother, Nasrin Rashid, for her continuous support and motivation for the timely completion of my work.

Contents

| | |
|--|-------------|
| Certification | ii |
| Candidate’s Declaration | iii |
| Dedication | iv |
| List of Figures | viii |
| List of Tables | xii |
| Acknowledgement | xiii |
| Abstract | xiv |
| 1 Introduction | 1 |
| 1.1 Preface | 1 |
| 1.2 Literature Review | 2 |
| 1.2.1 InGaN Nanowire-Based LED Devices | 2 |
| 1.2.2 AlGaN Nanowire-Based LED Devices | 3 |
| 1.2.3 Optical Light Polarization of III-Nitride LEDs | 5 |
| 1.3 Motivations | 5 |
| 1.4 Objectives of the Thesis | 7 |
| 1.5 Thesis Outline | 7 |
| 2 Thoretical Background | 9 |
| 2.1 Light Extraction Efficiency (LEE) of LED | 9 |
| 2.2 Nanowire-Based and Micro LEDs | 10 |
| 2.3 UV-Visible LEDs | 10 |
| 2.4 InGaN-Based LEDs and Applications | 11 |
| 2.5 AlGaN-Based LEDs and Applications | 11 |
| 2.6 Degree of Polarization | 12 |
| 2.7 DOP Calculation Methodology | 13 |
| 2.8 Parametric dependence on LEE | 14 |

| | | |
|----------|---|-----------|
| 2.9 | LEE Enhancement Methods of GaN LED devices | 15 |
| 2.9.1 | Surface Roughening | 16 |
| 2.9.2 | Substrate Engineering | 17 |
| 2.9.3 | Surface-plasmon enhanced LEDs | 18 |
| 3 | Simulation Framework, Methodology, and Structural Modeling | 19 |
| 3.1 | FDTD Simulation | 19 |
| 3.2 | Maxwell's Equations and the FDTD Method | 19 |
| 3.3 | Modeling LED Structures | 22 |
| 3.3.1 | Nanowire LED Structures | 22 |
| 3.3.2 | Planar Micro LED Devices | 24 |
| 3.4 | Simulation Setup | 24 |
| 3.4.1 | Single Nanowire LED Structure | 24 |
| 3.4.2 | Periodic Nanowire Array Structure | 26 |
| 3.4.3 | 2D Simulations for Planar Micro LED Structures | 27 |
| 3.4.4 | Structure with inclined reflectors | 27 |
| 3.5 | Degree of Polarization and LEE calculation using DOP | 28 |
| 3.5.1 | Weighted Average Method | 28 |
| 3.5.2 | Polarization Angle Method | 30 |
| 4 | Impact of Nature of Polarization and Nanowire Dimension on LEE | 32 |
| 4.1 | LEE of InGaN-Based LEDs | 32 |
| 4.1.1 | Structural Composition of InGaN nanowire LED | 32 |
| 4.1.2 | Side and Top Extraction for TE and TM Polarizations | 33 |
| 4.1.3 | Effect of Waveguiding Modes on Extraction Characteristics | 35 |
| 4.2 | LEE of AlGaN LEDs Operating at DUV | 36 |
| 4.2.1 | Side and Top Extraction Efficiencies for TE and TM Polarizations | 37 |
| 4.2.2 | Comparison of Extraction Efficiencies between TE and TM polarizations | 39 |
| 4.2.3 | LEE of InGaN Micro LEDs | 40 |
| 5 | LEE Calculation Using Degree of Polarization | 42 |
| 5.1 | LEE of InGaN LEDs Considering DOP | 43 |
| 5.1.1 | DOP Variation with Wavelength | 44 |
| 5.2 | LEE of AlGaN-Based DUV LED Considering DOP | 46 |
| 5.2.1 | Effect of DOP Variation | 49 |
| 5.2.2 | Effect of DOP Variation with Wavelength | 49 |
| 6 | Effect of Array Periodicity | 53 |

| | | |
|----------|--|-----------|
| 6.1 | InGaN LEDs | 53 |
| 6.2 | AlGaN-Based Nanowire LEDs | 56 |
| 7 | LEE Improvement | 58 |
| 7.1 | Influence of Bottom Metal Plate for Single InGaN nanowire | 58 |
| 7.2 | Effect on AlGaN-based single nanowire LED | 59 |
| 7.3 | Effect of Inclined Side Reflector on InGaN Nanowire Array LED | 60 |
| 7.4 | Effect of Inclined Side Reflector on AlGaN Nanowire Array and Micro LEDs | 61 |
| 7.5 | Comparison among different enhancement methods | 62 |
| 8 | Conclusions | 64 |
| 8.1 | Conclusions | 64 |
| 8.2 | Future Potentials of this Research Work | 65 |
| | References | 67 |

List of Figures

| | | |
|-----|--|----|
| 1.1 | (a) PL spectra (normalized) at 300K of multi-colour nanowire LED sub-pixels monolithically grown on Si substrate. (b) Multi-colour nanowire LED devices on the same chip [22]. | 2 |
| 1.2 | An example of InGaN/GaN nanowires LEDs where InGaN disks are shown schematically in GaN nanowires grown on a 200 nm thick Silica substrate. A 12 nm thick GaN spacer separates the two 2 nm thick InGaN disks. [23]. | 3 |
| 1.3 | (a) Schematic illustration of a single nanowire AlGaN deep UV LEDs. (b) A large-scale SEM image of AlGaN nanowires [34]. | 4 |
| 1.4 | (a) Schematic illustration of AlGaN deep UV LEDs fabricated on Si substrate coated with Al [39]. | 5 |
| 1.5 | Degree of polarization (DoP) as a function of the aluminium mole percentage in the QW, as determined by k-p calculations (dashed green), photoluminescence, and electroluminescence (violet circles, orange squares). The error bars show the observed value's standard deviation and its 20% underestimation as a result of light scattering processes. [43]. | 6 |
| 2.1 | A schematic representation of an experimental setup for analyzing optical polarization of emission. [44]. | 13 |
| 2.2 | Experimentally reported DOP for different MQW LEDs [44]. | 13 |
| 2.3 | (a)-(d) Schematics of InGaN QW LEDs with SiO ₂ / Polystyrene (PS) microlens array where PS thickness is varied [71]. | 14 |
| 2.4 | Various techniques employed for LEE enhancement in recent years [74]. | 15 |
| 2.5 | (a) SEM image of LED device with micro dome and nanorod hierarchical structures. (b) L-I curve and (c) EQE with current for three different surfaces [74]. | 16 |
| 2.6 | (a) SEM image and (b) schematic of a syringe-like ZnO nanorods [82]. . | 17 |
| 2.7 | (a) IQE and (b) EQE with current density for nanopatterned substrate LEDs and reference LEDs [84]. | 18 |
| 2.8 | LED devices with (a) embedded nanoparticles in n-GaN and (b) nanoparticles in etched p-GaN layer to couple QW-SP [74]. | 18 |

| | | |
|------|--|----|
| 3.1 | Representation of a standard Yee cell used in FDTD method illustrating how electric and magnetic field vectors are distributed [86]. | 20 |
| 3.2 | Different steps in the FDTD method in the form of a flowchart. [87]. . . | 21 |
| 3.3 | Schematic of (a) radial QW and (b) axial QW nanowire-based LED structures, and (c) three different dipole polarizations in a cylindrical nanowire. [11]. | 23 |
| 3.4 | Schematic of a longitudinal cross-section of two different types of nanowire LED structures: (a) InGaN/GaN MQW based nanowire LED structure and (b) AlGaIn MQW based nanowire LED structures showing material compositions. | 23 |
| 3.5 | Schematic of cross-section of InGaN/GaN MQW based planar micro LED devices showing material compositions. | 24 |
| 3.6 | Simulation setup for LEE calculation of nanowire-based LED devices. (a) Perspective view showing nanowire structure, dipole source, simulation region, boundary layers, and output power monitors. (b) Planar cross-sectional view of the simulation setup showing input power monitors inside the nanowire for measuring the dipole source power. | 25 |
| 3.7 | A schematic representation of a nanowire-array based LED devices [11]. | 26 |
| 3.8 | A unit cell for simulating nanowire periodic arrays indicating boundary conditions and top extraction plane. | 27 |
| 3.9 | A schematic of a micro LED device with top and side extraction lines for calculating top and side extraction. | 27 |
| 3.10 | A schematic showing a periodic nanowire array arrangement with inclined sidewall reflector for enhancing the top extraction. | 28 |
| 3.11 | A schematic showing the polarization angle of the dipole source with respect to TE and TM polarization. | 30 |
| 4.1 | Emission characteristics for TM and TE polarization. (a) Electric field distribution and (b) top, side and total extraction efficiencies for TM polarization. (c) Electric field distribution and (d) top, side and total extraction efficiencies for TE polarization. | 33 |
| 4.2 | . Comparison between (a) top and (b) side extraction efficiency for TE and TM polarization | 34 |
| 4.3 | Electric field intensity distribution of four lowest order guiding modes for a nanowire with a diameter of 200 nm. [88] | 35 |
| 4.4 | Top extraction efficiency for TE polarization. | 36 |
| 4.5 | Comparison between top and side extraction efficiency for TE polarization. | 36 |

| | | |
|-----|--|----|
| 4.6 | Top, side and total extraction efficiencies of UV-C AlGaIn nanowire LEDs for (a) TM polarization and (b) TE polarization. | 37 |
| 4.7 | E-field pattern showing superior side and total extraction efficiencies for specific diameter. Electric field distribution for TE polarization for diameter (a) 130 nm and (b) 190 nm. | 38 |
| 4.8 | (a) Top, (b) side and (c) total extraction efficiency for both TE and TM polarizations. | 39 |
| 4.9 | Top, side and Total extraction efficiencies of micro-LED devices for (a) TM polarization, (b) TE polarization. | 40 |
| 5.1 | Degree of Polarization (DOP) with emission wavelength for (a) InGaIn-based LED operating in the wavelength range of 390-460 nm and (b) different group III-Nitride LEDs. [47, 89] | 42 |
| 5.2 | Calculation of LEE of InGaIn nanowire LED using DOP values. (a) Top, (b) side, and (c) total extraction for DOP = 0.6 at a wavelength of 400 nm. | 43 |
| 5.3 | Top Extraction at (a) 400 nm and (b) 457 nm for InGaIn nanowire LED and (c) comparison between the top efficiencies for these two wavelengths. Side Extraction at (d) 400 nm and (e) 457 nm for InGaIn nanowire LED and (f) comparison between the side efficiencies for different wavelengths. (g) Comparison between the total efficiencies for 400 nm and 457 nm wavelengths. | 45 |
| 5.4 | Effect of DOP variation with wavelength. (a) top, (b) side and (c) total extraction efficiencies considering DOP values for emission wavelength at 400 nm, 410 nm, 415 nm, 447 nm and 457 nm. | 46 |
| 5.5 | (a), (b) Degree of polarization calculated from in-plane electroluminescence as a function of wavelength for several group III-Nitride LEDs. (c) Optical intensity of in-plane emission for different group III-nitride LEDs [44, 89]. | 47 |
| 5.6 | Calculation of LEE of AlGaIn nanowire LED using DOP values. (a) Top, (b) side, and (c) total extraction for DOP = -0.4 at a wavelength of 250 nm. | 48 |
| 5.7 | (a) Top, (b) side and (c) total extraction efficiency considering DOP values of -0.4, -0.3 and -0.15, respectively. | 49 |

| | | |
|-----|---|----|
| 5.8 | Top Extraction at (a) 250 nm and (b) 320 nm for AlGaIn nanowire LED and (c) comparison between the top efficiencies for different wavelengths. Side Extraction at (d) 250 nm and (e) 320 nm for AlGaIn nanowire LED and (f) comparison between the side efficiencies for different wavelengths. (g) Comparison between total extraction efficiencies for 250 nm and 320 nm wavelengths. | 50 |
| 5.9 | Effect of DOP variation with wavelength. (a) top, (b) side and (c) total extraction efficiencies considering DOP values for emission wavelength at 250 nm, 290 nm, 310 nm and 320 nm. | 51 |
| 6.1 | LEE on top for different InGaIn nanowire diameters and distances for (a) TM polarization, (b) TE polarization, and (c) considering DOP. . . . | 54 |
| 6.2 | Electric field pattern (TM polarization) for diameter = 50 nm and (a) distance = 100 nm, (b) distance = 400 nm. Radiation pattern for diameter = 350 nm and (c) distance = 150 nm and (d) distance = 400 nm. . . . | 55 |
| 6.3 | Electric field pattern (TE polarization) for (a) diameter = 50 nm, distance = 100 nm, and (b) diameter = 150 nm distance = 150 nm. Radiation pattern for (c) diameter = 150 nm, distance = 400 nm and (d) diameter = 50 nm, distance = 400 nm. | 56 |
| 6.4 | LEE on top for AlGaIn-based LEDs for different nanowire diameters and distances for (a) TM polarization, (b) TE polarization, and (c) considering DOP. | 57 |
| 7.1 | A schematic of single InGaIn nanowire LED with bottom Al metal plate for LEE enhancement. | 59 |
| 7.2 | Percentage LEE enhancement due to the introduction of bottom reflector. | 59 |
| 7.3 | Radiation pattern for InGaIn-nanowire array-based micro LEDs for TM polarization (a) without and (b) with inclined sidewall reflectors. Emission pattern for TE polarization (c) without and (d) with inclined side reflectors. | 60 |
| 7.4 | Percentage LEE enhancement with inclination angle of the sidewall reflectors. | 61 |
| 7.5 | Emission pattern for AlGaIn micro UV-C LEDs with inclined Al side reflectors for (a) TM polarization and (b) TE polarization [56] | 62 |

List of Tables

| | | |
|-----|---|----|
| 4.1 | For a dielectric cylinder with $\epsilon = 6.25$ in air, the cutoff values for several lowest order modes [88] | 35 |
| 5.1 | DOP and the ratio of TE and TM polarization intensities for several emission wavelengths for InGaN-based LED devices [47]. | 43 |
| 5.2 | DOP and the ratio of TE and TM polarization intensities for several emission wavelengths for AlGaIn-based LED devices [90]. | 47 |
| 7.1 | Comparison among different LEE enhancement methods. | 62 |

Acknowledgement

First and foremost, I am very grateful to the Almighty for giving me the strength to successfully and timely complete my thesis.

I am highly indebted to my thesis supervisor, Dr. Md. Zunaid Baten, Associate Professor, Department of Electrical and Electronic Engineering (EEE), Bangladesh University of Engineering and Technology (BUET), for his constant supervision, guidance and motivation. The last year and a half have been very challenging for me as I had to balance multiple things simultaneously and felt quite overwhelmed at times. But, his constant support, timely advice, and encouragement helped me navigate difficult situations while making research progress.

I want to express my gratitude towards Dr. Md Aynal Haque, Dr. Sharif Mohammad Mominuzzaman, Dr. Sajid Muhaimin Choudhury, and Dr. Mainul Hossain for giving their consent to be a part of my board of examiners. I am also extremely thankful to my collaborators, especially Sharif Md Sadaf, for the publication of a part of my thesis work in a top-notch journal like ACS Photonics. Through this collaboration, I learnt about LED device fabrication in addition to optical simulations, and this research work has sparked my interest in experimental research. I am also appreciative of the contribution of the Electrical and Electronic Engineering department, BUET, to the successful completion of my thesis.

I would also like to thank my friends and colleagues at the EEE department for their continuous motivation and encouragement. Last but not least, I am extremely grateful to my family members, especially my mother, whose tireless effort and unconditional love made my life much easier and helped me concentrate on my research work.

Abstract

Nanowire array-based III-nitride micro LEDs operating from UV to visible range have attracted tremendous attention for many photonics and optoelectronics applications. However, traditionally, these LEDs' light extraction efficiency (LEE) is numerically evaluated without considering specific optical polarization characteristics. In this thesis, we evaluated the LEE of III-nitride UV and visible single nanowire LEDs, a periodic array of nanowire emitters, and micro LEDs considering Degree of Polarization (DOP) using FDTD-based optical simulations. We proposed a weighted average method for calculating LEE considering DOP from LEE values obtained for TE and TM polarizations. The influence of emission polarization on the side and top LEE of single InGaN and AlGaN nanowire LEDs were studied and analyzed using waveguiding nature of these nanowire structures. The impact of structural parameters was also studied extensively. Considering DOP and material absorption, the maximum calculated top, side and total extraction efficiencies for a single AlGaN nanowire LED operating at 250 nm are 11.4%, 75.8% and 87.3%, respectively. Similarly, for a single InGaN nanowire-based LED operating at 400 nm, the maximum top extraction efficiency of 30% is achieved for a nanowire diameter of 125 nm. Here, we have also analyzed the impact of DOP variation on the overall efficiency characteristics. Moreover, a comprehensive study has been conducted on the dependence of LEE on various structural parameters such as nanowire diameter and array periodicity considering DOP. We also proposed an optimized geometry for the InGaN and AlGaN periodic nanowire array LED structures for maximizing top extraction efficiencies. Considering DOP, we achieved the maximum top extraction of 67% for InGaN nanowire array-based micro LEDs for nanowire diameter and array periodicity of 50 nm and 350 nm, respectively. Additionally, in this work, we have analyzed two methods for LEE enhancement: insertion of inclined side reflectors and bottom metal reflectors. For InGaN single nanowire LED, we demonstrated LEE enhancement of 28%, with the insertion of a 50 nm thick bottom Al reflector layer. We also studied the influence of inclined side wall reflectors on the enhancement of top extraction efficiencies for nanowire array-based micro LEDs and planar micro LEDs. Using our optimized geometry and taking DOP into consideration, the enhancement of top LEE for InGaN nanowire array-based LED devices with inclined side reflectors having an inclination angle of 30 degrees was calculated to be 90

Chapter 1

Introduction

1.1 Preface

Micro and nanowire array-based III-nitride semiconductor LEDs operating from UV to visible range have gained interest for a number of applications related to photonics and optoelectronics in recent years [1–6]. Especially, LEDs based on GaN materials have recently attracted tremendous attention in the fields of solid-state lighting, liquid crystal displays and many others [7–10]. Compared to conventional lighting systems, these solid-state systems are smaller in size, more durable and quick in response time [11]. GaN-based visible LEDs are already being used in displays, lamps, picture projectors and efficient light sources [12, 13]. Additionally, AlGaN material-based UV LEDs are gaining interest for potential applications in areas related to water and air purification, disinfection and sterilization [14, 15]. However, the major limiting factor for these LED devices is the poor light extraction efficiency (LEE) which limits the overall external quantum efficiency and nanowire structures with embedded QWs and QDs as single-photon-sources are promising candidates for highly efficient semiconductor LEDs [16, 17]. Several advantages of nanowires in optoelectronic applications are smaller size, strong mode confinement, waveguiding nature, and directional emission [18]. These characteristics originating from specific nanowire geometry contribute to the enhancement of overall extraction efficiencies for nanowire-based LEDs.

1.2 Literature Review

1.2.1 InGaN Nanowire-Based LED Devices

Recently, InGaN-based LEDs have attracted a lot of attention for applications in display devices, lighting systems, visible light communication (VLC) in smart lighting systems, plastic optical fibre (POF) communication and underwater wireless optical communication (UWOC) [19]. The large band gap of InGaN has made it an attractive candidate for tunable LEDs and lasers operating in a broad wavelength range. However, growing InGaN compounds with high In content and low density of dislocations can be extremely difficult. Here, nanowire geometry has a unique advantage of strain relieving property which contributes to higher quantum efficiency [20]. Furthermore, this nanowire geometry also results in an enhancement of extraction efficiency and a reduction in overall light absorption. However, enhancing the extraction efficiency is still a challenge for these LED devices to be widely used and commercialized. Using halide chemical vapour deposition (HCVD), Hahn et al. demonstrated the growth of InGaN nanowires on a sapphire substrate [20]. In this work, they also demonstrated tunable emission ranging from yellow to visible spectrum [20]. Guo et al. demonstrated InGaN/GaN nanowire LEDs grown on Si substrate using molecular beam epitaxy (MBE). The emission wavelength has been tuned from UV to red by varying the composition [21]. Similarly, Wang et al. demonstrated full-colour light generation using InGaN nanowires. Different colour LEDs were monolithically integrated on a Si substrate. The growth process comprises three steps of selective area MBE [22].

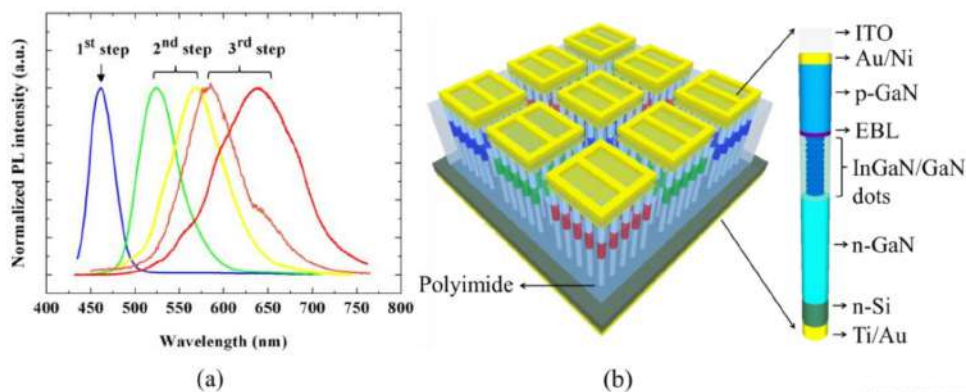


Figure 1.1: (a) PL spectra (normalized) at 300K of multi-colour nanowire LED subpixels monolithically grown on Si substrate. (b) Multi-colour nanowire LED devices on the same chip [22].

Several other fabrication methods and applications of InGaN LEDs are reported in the literature. Rashidi et al. demonstrated the use of InGaN/GaN LEDs in VLC (visible

light communication). They fabricated the high-speed LED devices on nonpolar GaN substrates [19]. Park et al. using plasma assisted-MBE, fabricated GaN nanowires with InGaN disks on SiO₂ layer [23]. Besides LED fabrications, several optical simulation works have been undertaken for calculating the extraction efficiencies which also impact the external quantum efficiency and overall LED power conversion efficiency. Ryu et al. has calculated the light extraction efficiency (LEE) of InGaN LEDs using 3D FDTD simulations. They exhibited the use of photonic crystals and reflective layer in LEE enhancement and also analyzed the structural dependence on LEE [24]. Zhu et al. introduced microsphere arrays in top InGaN LEDs for improving LEE and calculated the enhancement factor of 2 using optical simulations [25].

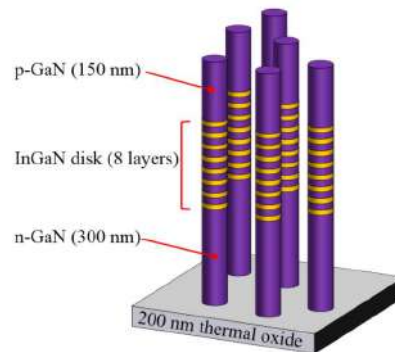


Figure 1.2: An example of InGaN/GaN nanowires LEDs where InGaN disks are shown schematically in GaN nanowires grown on a 200 nm thick Silica substrate. A 12 nm thick GaN spacer separates the two 2 nm thick InGaN disks. [23].

1.2.2 AlGaN Nanowire-Based LED Devices

Due to direct and modifiable bandgap energies, AlGaN nanowires have become attractive candidates for mid-deep UV (207 to 364 nm) light-emitting diodes (LEDs) and lasers [26–28]. The AlGaN nanowires for nanowire-based UV light-emitting diodes are generally fabricated using methods such as molecular beam epitaxy (MBE) and metalorganic chemical vapour deposition (MOCVD). Moreover, optical and electrical properties for these nanowires grown on different substrates/ templates are analyzed in detail [29]. Traditionally, various applications of UV- light technologies for disinfection, curing and sensing relied on poisonous and hazardous mercury lamps but nowadays, semiconductor UV-light technologies are poised to displace these traditional technologies [29, 30]. Using CVD and Physical vapour deposition (PVD) methods, a wide range of Al content in AlGaN nanowires has been demonstrated [5, 31]. Several large-scale epitaxial methods, such as MOCVD and metalorganic vapour phase epitaxy (MOVPE) have been employed to fabricate large-area AlGaN nanowire UV LEDs. Al-

GaN nanowires have been grown on patterned substrates in order to achieve higher uniformity using several selective area growth methods [32,33].

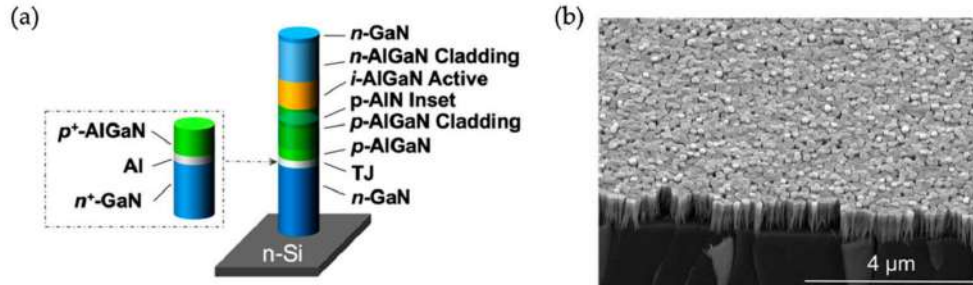


Figure 1.3: (a) Schematic illustration of a single nanowire AlGaIn deep UV LEDs. (b) A large-scale SEM image of AlGaIn nanowires [34].

There have been many studies where the electrical and optical characteristics of ternary compound AlGaIn nanowires grown on Si substrate have been extensively studied [35]. Despite having several advantages, AlGaIn nanowires grown on Si substrate suffer from some major drawbacks, such as high absorption in the UV range and generation of a barrier layer limiting electronic transport [35]. Researchers have demonstrated AlGaIn nanowires grown on metal-coated and metal-foil substrates. Hoiass et al. demonstrated AlGaIn nanowire UV-LEDs grown on graphene-coated glass substrate [36]. Previously, it has been reported that AlGaIn nanowires having GaN/AlGaIn active regions have been grown on patterned GaN-on-sapphire templates [33]. Several studies have also been conducted on nonpolar AlGaIn nanowire LEDs due to enhanced device performance. Coulon et al. first demonstrated nonpolar single AlGaIn QW grown on AlN using MOCVD [37]. Core-shell nonpolar AlGaIn UV LED structures with very high intensity using MBE have also been reported [38].

Due to high absorption in the UV range and dominant TM polarization nature, UV LEDs suffer from low light extraction efficiencies. Hence, many simulation studies proposing different structural parameters, device designs, and materials in order to enhance LEE have been reported [40–42]. In order to reduce light absorption in the top metal layer, a nanowire array with graphene electrodes has been proposed and optical simulations have been employed to investigate the effect of structural parameters on the extraction values [40]. Ryu et al. demonstrated a large enhancement of LEE through optimizing structural parameters using FDTD simulations [41].

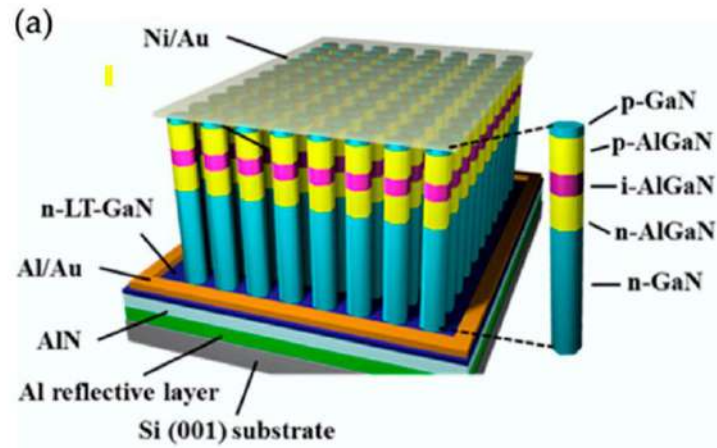


Figure 1.4: (a) Schematic illustration of AlGaN deep UV LEDs fabricated on Si substrate coated with Al [39].

1.2.3 Optical Light Polarization of III-Nitride LEDs

Optical polarization of III-Nitride LED devices has been studied extensively due to its contribution to radiation pattern and extraction efficiency. Guttman et al. extensively studied the polarization nature and LEE of AlGaN UV LEDs and demonstrated a transition from dominant TE to dominant TM polarization nature with increasing Al mole fraction in the MQW. They also demonstrated the effect of this transition on the overall extraction efficiency using ray tracing methods [43]. This transition actually results from a negative crystal field changing the valence band order and oscillatory strength. Kolbe et al. experimentally analyzed the optical polarization nature of (In)(Al)GaN MQW LEDs operating in the UV-A and UV-B range [44]. Shakya et al. reported the polarization nature of blue and ultraviolet LEDs based on III-Nitride materials using polarization-resolved electroluminescence study. They found a degree of polarization 0.29 for edge-emitting blue LEDs and almost 0.4 for UV LEDs [45]. Reich et al. also reported strong TE-polarized emission from AlGaN QW deep UV LEDs using narrow QW and barriers with high Al content [46]. Jia et al. investigated the optical polarization nature for InGaN/GaN MQW LEDs operating in the wavelength range from 395-455 nm [47].

1.3 Motivations

Traditionally, the light extraction efficiency of LEDs is evaluated and reported using optical simulations, considering specific polarization of the light emitter [48, 49]. However, as mentioned earlier, it has been experimentally demonstrated that the emission

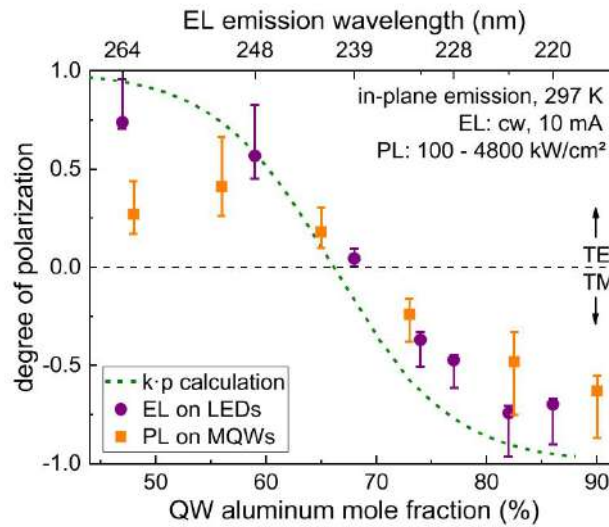


Figure 1.5: Degree of polarization (DoP) as a function of the aluminium mole percentage in the QW, as determined by k-p calculations (dashed green), photoluminescence, and electroluminescence (violet circles, orange squares). The error bars show the observed value's standard deviation and its 20% underestimation as a result of light scattering processes. [43].

polarization characteristic of III-nitride LEDs is not purely transverse electric (TE) or transverse magnetic (TM) in nature, but rather a mixture of both [43, 45]. So in order to accurately estimate the LEE of these LEDs using optical simulations, the degree of polarization (DOP) should be duly taken into consideration. As the demand for highly efficient solid-state lighting technology is increasing, the accurate estimation of LEE has become an urgent need. In this thesis, we evaluated the extraction efficiencies of nanowire and micro LEDs considering optical polarization characteristics and this method of LEE evaluation can be generalized for other LED devices. Additionally, even though the DOP values have been reported to vary with emission wavelength, the impact of this variation on overall efficiency is yet to be explored. Moreover, a detailed study on the impact of emission polarization on the side and top extraction of LEDs operating at UV and visible range is currently missing in the literature. Moreover, it is known that the LEE of nitride nanowire LEDs depends on various structural parameters, such as nanowire diameters, aspect ratio and array periodicity [11, 41]. Hence a comprehensive study considering material absorptions, device dimensions, array order, and DOP is necessary to explore the design space of these devices in order to maximize their light extraction efficiency. In this work, we also explored and analyzed the impact of these complex variables on overall efficiency.

Based on the findings of this design space, it is necessary to systematically investigate and compare different techniques for enhancing the LEE of these highly prospective

optoelectronic devices. In this work, two methods: metal reflectors and inclined reflectors, have been introduced and their impact on LEE improvement considering optical polarization characteristics have been critically analyzed.

1.4 Objectives of the Thesis

The objectives and specific aims of this work are the following:

- i. To analyze the effect of emission polarization nature on top and side extraction efficiency of nitride nanowire and micro LEDs.
- ii. To evaluate the top and side extraction efficiency of micro and nanowire array-based LEDs taking into consideration the wavelength dependence of DOP.
- iii. To optimize the structural parameters, such as diameter and array periodicity, to attain maximum LEE while taking into consideration emission polarization, material absorption and waveguiding.
- iv. To investigate different techniques, such as the insertion of bottom metal plates and inclined reflectors, to enhance the light extraction efficiency of the optimized device.

1.5 Thesis Outline

The rest of this thesis is outlined as follows:

Chapter 2 deals with the theoretical background of the research work. This chapter begins with the definition of light extraction efficiency (LEE) of LEDs and discusses nanowire and micro InGaN and AlGaIn LED structure and applications in the first half. The next sections of this chapter deal with optical polarization characteristics of emission, and parametric dependence on LEE. Finally, several methods employed for LEE enhancement are introduced in the last section.

Chapter 3 discusses the simulation framework used, the methodology adopted and the structural modelling used throughout this thesis. In the first half of the chapter, Maxwell's equation and how it is numerically solved using FDTD techniques have been discussed. This chapter also shines a light on nanowire array-based and micro LED devices in a bit more in detail. Simulation set-up for different configurations and

methods used for LEE calculation is also described in this section. In the final section, we mention the methods used for calculating LEE considering optical polarization characteristics.

Chapter 4 contains the impact of LEE on the nature of optical polarizations, and structural dimensions. This section discusses how side and top extraction of isolated single InGaN and AlGaN nanowire LEDs are impacted by emission polarization considering the waveguiding characteristics of the nanowire structure. Moreover, the effect of structural parameters on the overall extraction is also studied extensively in this chapter.

In Chapter 5, we calculate the LEE of nanowire-based and micro InGaN and AlGaN LED devices considering the degree of polarization (DOP). The impact of DOP variation with emission wavelength on LEE is also studied in this chapter. This chapter also compares the extraction efficiencies with and without considering DOP.

Chapter 6 introduces a periodic nanowire array of emitters replacing isolated single nanowire and the LEE of this periodic nanowire array is evaluated. The influence of nanowire dimensions and distance between the nanowires on the LEE is studied and analyzed in detail for both UV and blue LEDs. Finally, an optimized geometry is proposed for maximizing the top extraction efficiencies of these LEDs.

Chapter 7 deals with several proposed methods for the enhancement of nanowire and micro LED devices. The influence of a bottom Al metal reflector for single nanowire AlGaN and InGaN LEDs is discussed in detail and enhancement factors are reported. Moreover, the effect of inclined Al side-reflectors in periodic nanowire arrays and micro LEDs on LEE is also reported in the last half of this chapter.

Chapter 8 contains the concluding remarks and mentions some possible future research work based on this thesis.

Chapter 2

Thoeretical Background

In this chapter, we introduce the required theoretical background of this thesis. We also elaborate on the light extraction efficiency (LEE) of LED devices and highlight various nanowire-based and micro LEDs. We specially focus on InGaN-based LEDs operating in the visible wavelength and AlGaIn-based LEDs operating in the UV region. We also introduce the concept of degree of polarization (DOP) in this chapter and discuss the experimental set-up used to evaluate DOP. Finally, we briefly mention some of the parameters affecting LEE performance and some methods related to LEE enhancement.

2.1 Light Extraction Efficiency (LEE) of LED

Light Extraction Efficiency (LEE) of a LED is a measure of how much light that is generated inside the LED device is extracted outside. LEE is defined as [50]

$$\text{LEE} = \frac{\text{Number of photons emitted into free space per second}}{\text{Number of photons emitted from active region per second}} = \frac{P/(hv)}{P_{\text{int}}/(hv)}. \quad (2.1)$$

Where P is the optical power extracted outside, P_{int} is the optical power emitted from the active region of the LED, h is the Plank's constant and v is the frequency of the photon.

Besides theoretical calculation, LEE is traditionally evaluated through performing optical simulations [51, 52]. LEE is an important performance parameter and the overall efficiency of LED devices greatly depends on the extraction efficiency. Poorer extraction efficiency results in an inefficient, dimmer LED and hence, significant attention has been given to enhancing the extraction performance. There are several factors that affect LEE such as the refractive index of the material and surrounding media, reflectivity

of the surfaces, shape and size of the device, and material absorption [53, 54]. Several techniques such as texturing surfaces, introducing photonic structures, metal plates and inclined sidewalls have been employed to increase LEE [55–57].

2.2 Nanowire-Based and Micro LEDs

Micro LEDs are very small in size and individual pixels can be made of a single LED having a size of less than 100 micrometres. In advanced micro LED-based display technology, a large number of miniaturized LEDs create an image, resulting in a much higher resolution and pixel density. Micro LEDs have garnered tremendous attention in display research in recent years as it exhibits tremendous performance in terms of efficiency, brightness, lifetime and resolution [58–60]. Micro LEDs are perfect candidates for outdoor applications due to high brightness. Additionally, due to high efficiency, they consume much less power than traditional display devices. It has recently found tremendous success in virtual reality, consumer electronics, and high-quality displays. Micro LEDs can also be fabricated in flexible substrates so they can be used in wearable technology [61]. Moreover, researchers have made tremendous progress in applying these devices to medical devices, optogenetics, and sensors [62, 63].

A nanowire array-based LED devices have an array of nanowires with active regions that emit light. These nanowires usually have diameters less than 100 nm and thus they can be very useful in high-resolution and pixel-density display devices. Traditionally, these nanowires are composed of semiconductor materials and grown vertically on the substrate. An advantage of these nanowire LEDs compared to micro-LEDs is the presence of a large surface area which may result in higher extraction efficiency. However, maintaining uniformity in dimension and spacing, cost of fabrication and several other complexities are yet to be solved. Still, due to compact size, flexibility and high extraction efficiency, nanowire LEDs have the potential to revolutionize display, and healthcare industries and replace traditional devices [64, 65].

2.3 UV-Visible LEDs

There are several semiconductor LEDs operating in a wavelength range from UV to visible. UV semiconductor LEDs are composed of Gallium Nitride (GaN) and Aluminum Gallium Nitride (AlGaN) materials. On the other hand, LEDs operating in the visible spectra are made from materials such as Gallium Nitride (GaN), Indium Gallium Ni-

tride (InGaN), Aluminum Gallium Indium Phosphide (AlGaInP), Aluminum Gallium Arsenide (AlGaAs), and Silicon Carbide (SiC). In this work, we mainly focused on AlGaN-based UV LEDs and InGaN-based LEDs operating in the visible region.

2.4 InGaN-Based LEDs and Applications

InGaN-based LED technology is relatively more mature than compared to AlGaN UV LEDs. These LEDs emit light in the range of 400-550 nm [66]. Here, the In content in the InGaN composition dictates the bandgap and hence the emission wavelength. InGaN LEDs have found significant applications in high-intensity blue and green light. As a result, they are widely used in solid-state lighting and display technologies, automotive lighting. In medical applications, blue LEDs have been used in photodynamic therapy to treat complicated medical conditions. These LEDs are also extensively used in sensing and detection. Researchers are also working on finding new potential applications for these LED devices in biotechnology, environmental sensing, and communication. Just like any other emerging technology, InGaN LED technology also has some limitations. “Efficiency droop”- the reduction of efficiency at high current density- is a limiting factor. Another shortcoming of these LEDs is that the emission wavelength shifts to a lower wavelength at higher currents. The temperature sensitivity, crystal defects and cost of fabrications are still posing great challenges. Ongoing research is focused on overcoming these challenges and improving efficiency, output power, and reliability.

2.5 AlGaN-Based LEDs and Applications

Aluminum Gallium Nitride (AlGaN) Light Emitting Diode emits light in the wavelength range from UV to blue spectrum. The change in the bandgap and hence the emission wavelength is dependent on the content of Al in the composition. It has been experimentally demonstrated that AlGaN-based LEDs can emit light in the range from 250 to 450 nm [67]. Several epitaxial growth techniques, such as metal-organic chemical vapor deposition (MOCVD) or molecular beam epitaxy (MBE) have been employed to grow these LED devices with precise composition and structure [68, 69]. Each layer of the LED device has a different composition and thickness. The techniques are meticulously tuned for precise structural composition. There is also ongoing research which is focused on optimizing the fabrication techniques. Due to their high brightness and longer lifetime, these LEDs have found applications in many different fields. More-

over, they are also ideal for potential applications in sterilization, lighting, semiconductor manufacturing and display. AlGaN LEDs have been used to disinfect and sterilise air and water purification systems and food processing. Moreover, these LEDs have also found applications in indoor farming and plant research. In the semiconductor manufacturing industry where high-intensive UV emission is required for photolithography, AlGaN LEDs have huge potentials. These devices have also been used in blue and white lighting and display. Additionally, the shorter emission wavelength of these LEDs makes them perfect for sensing and detection. These AlGaN LEDs also suffer from some limitations. They have a limited emission wavelength range which limits their applications. Moreover, lower external quantum efficiency results in a lower overall efficiency and ongoing research efforts are focusing on improving the overall efficiency. Temperature sensitivity also severely limits potential applications. Most importantly, the cost is also a huge issue, as the fabrication of AlGaN LEDs is still quite expensive. However, AlGaN LEDs are still promising technology, and researchers are working tirelessly to improve efficiency, wavelength range and output power.

2.6 Degree of Polarization

The Degree of Polarization (DOP) is a measure of the relative strength of transverse electric (TE) and transverse magnetic (TM) polarized emission components. The DOP is defined by [46]

$$\text{DOP} = (I_{TE} - I_{TM}) / (I_{TE} + I_{TM}) \quad (2.2)$$

where I_{TE} and I_{TM} are the TE-polarized and TM-polarized light emission intensities, respectively.

As we can see, the DOP value can vary from -1 to 1. A DOP value of -1 indicates the purely TM nature of the emission, and a DOP value of 1 dictates the purely TE nature. When the polarization vector of the electric field (E) is perpendicular to the growth axis (c) of the structure, i.e. ($E \perp c$), then the polarization is defined as the TE polarization. Similarly, When the polarization vector (E) and the growth axis (c) are parallel, i.e. ($E \parallel c$), then the polarization is defined as the TM polarization. DOP actually denote the relative strength of each of these components and tells us the polarization nature of the emission. One thing to note here is that the emission polarization of these semiconductor LEDs is not purely TE or TM, but rather a mixture of both. The polarization nature is defined by the DOP. For example, the polarization nature of AlGaN LEDs

is mostly TM, which also limits the top extraction efficiency, and on the other hand, InGaN LED's emission polarization nature is mostly TE polarized as defined by a positive DOP value. In this work, we included the nature of polarization in our extraction efficiency calculation.

2.7 DOP Calculation Methodology

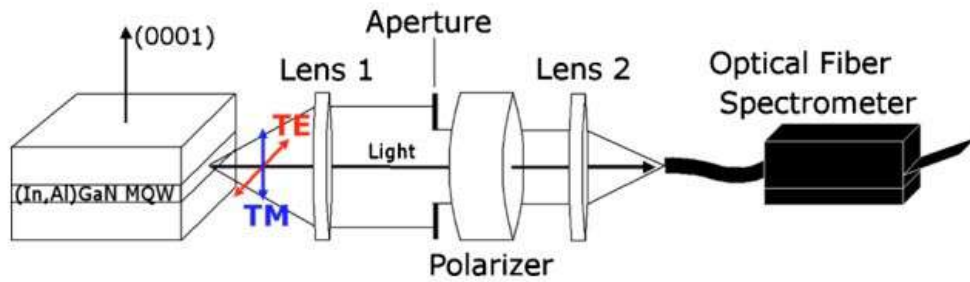


Figure 2.1: A schematic representation of an experimental setup for analyzing optical polarization of emission. [44].

A schematic of the experimental setup for analyzing polarization-resolved electroluminescence (EL) spectra is shown in Figure 2.1. The in-plane emission of the LEDs is shown in Figure 2.1. The in-plane emission of the LEDs is passed through the lens, aperture, and polarizer. The polarization-resolved emission is then coupled to an optical fibre and is eventually collected and analyzed by the spectrometer. The polarizer can be rotated to resolve TE and TM polarized emission.

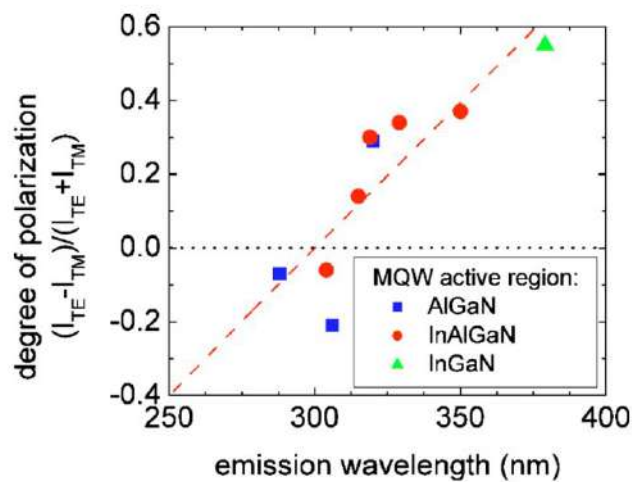


Figure 2.2: Experimentally reported DOP for different MQW LEDs [44].

Figure 2.2 demonstrates the dependence of the polarization nature on emission wavelength. For AlGaIn UV LEDs, below 310 nm, DOP has a negative value indicating the

dominant TM polarization nature. However, there is a shift from TM to TE polarized nature with emission wavelength as we observe that at 320 nm, the TE polarization component dominates. Moreover, this TM-dominant polarization nature of UV LEDs significantly reduces the extraction efficiency. It is also observed that, in the case of InAlGaN and InGaN-based blue LEDs, the emission is mainly TE in nature and the percentage of TE polarization increases with emission wavelength. This polarization characteristic also contributes to the relatively higher top extraction efficiencies of these blue LED devices. This dependence of DOP with the wavelength stems from the rearrangement of the band structure due to the compositional change.

2.8 Parametric dependence on LEE

Besides the polarization nature, the LEE of nanowire and micro LEDs depends on a number of parameters. A few of the major parameters are listed below:

Device Geometry and Structural Parameters: LEE is affected by the shape and the size of the devices [70]. For example, it has been reported that due to lower internal reflection, nanowires with tapered shapes have a higher light extraction efficiency. Furthermore, various structural parameters such as nanowire diameter, and array periodicity significantly impact the total extraction. Moreover, the structural dependence on the LEE stems from the modal characteristics inside the nanowires. In this study, we also explored the effects of these parameters in more detail.



Figure 2.3: (a)-(d) Schematics of InGaN QW LEDs with SiO_2 / Polystyrene (PS) microlens array where PS thickness is varied [71].

Optical Structures: Various optical structures such as micro-lenses (Figure 2.3) and

photonic crystals have been employed to enhance the total extraction efficiency [72].

Refractive index of the materials and surrounding: The refractive index of the LED structure and the surrounding medium dictate the reflection in the surfaces and hence LEE.

Substrate: The choice of the substrate on which the LED devices are grown also influences the LEE. Substrates with higher refractive index lower the LEE and substrates with lower refractive index enhance LEE by reducing the reflection.

Material Quality and Roughness: LEE also depends on the quality of the materials and surface roughness. A high-quality material with lower defect density and smoother surface can reduce the scattering and enhance extraction efficiency [73].

2.9 LEE Enhancement Methods of GaN LED devices

Enhancing the LEE of GaN LED devices is a topic of ongoing research, and many methods have been proposed to improve LEE as shown in Figure 2.4. Surface texturing has been proposed as a promising candidate for LEE enhancement. Moreover, the fabrication of LED devices on patterned sapphire substrates has been reported to improve extraction performance. Axial and core-shell nanorod structures have also been proposed for extraction and directional improvement. Recently, LED structures employing surface plasmons have also been employed to significantly boost extraction performance.

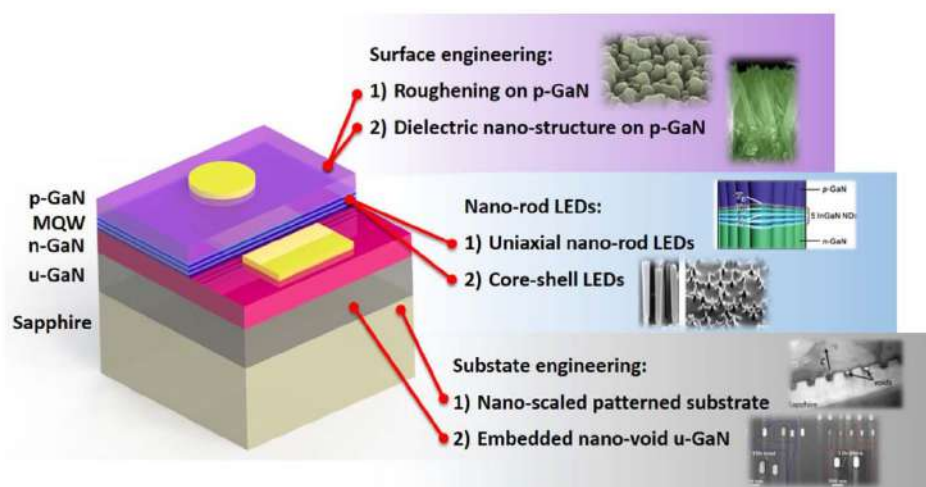


Figure 2.4: Various techniques employed for LEE enhancement in recent years [74].

2.9.1 Surface Roughening

A larger percentage of light can't be extracted outside GaN LED devices due to the TIR reflection at the GaN/air interface. This light is then absorbed by the LED device itself. Through surface engineering, the probability of light escaping the structure can be increased significantly. Several surface engineering techniques have been proposed to enhance extraction efficiency:

2.9.1.1 Roughening p-GaN layer

Many have reported LEE enhancement due to introducing micro/nano roughening on p-GaN layer [75, 76]. Introduction of nanospheres, nanoparticles on p-GaN surface layer has been reported to enhance scattering at the front facet and enhance vertical extraction. A design consisting of p-GaN micro dome structure (Figure 2.5(a)) and nanorod structure has resulted in LEE enhancement of 36.8% [74].

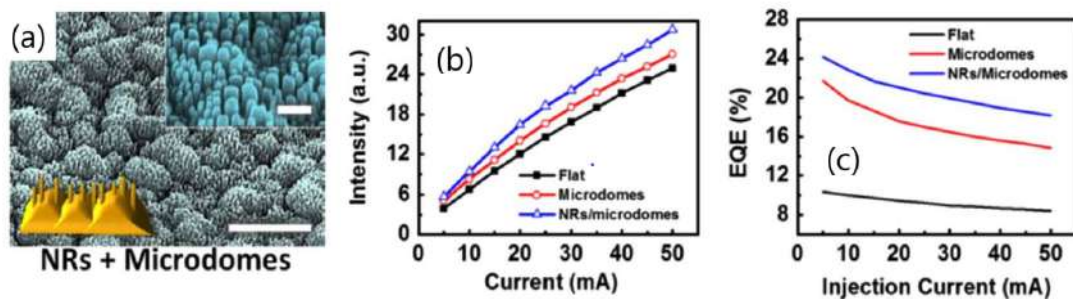


Figure 2.5: (a) SEM image of LED device with micro dome and nanorod hierarchical structures. (b) L-I curve and (c) EQE with current for three different surfaces [74].

2.9.1.2 Employing PC (Photonic Crystal) structure

Employing a PC structure on top of an LED device is a more advanced surface roughening strategy. Designing a photonic crystal structure with a specific bandgap can limit the lateral propagation of light and can lead to better LEE through waveguiding nature [72, 77, 78]. Furthermore, the introduction of PC can enhance the directional performance of the emitters, which can be extremely helpful for specific applications in projectors and display devices. However, fabrication PC structures require precise nanofabrication tools and these structures also suffer from current spreading. Chen et al. showed LEE enhancement of GaN LEDs by combining PC and material doping. The optimal LEDs have been reported to achieve LEE 19% and 14% for blue and UV LEDs, respectively [79].

2.9.1.3 Employing dielectric nano-structure on top of p-GaN

Inserting a dielectric material (Silica, ZnO, ITO) with a refractive index between GaN and air can significantly enhance the extraction efficiency of GaN LED devices (Figure 2.6). Ee et al. demonstrated 219% enhancement of light output power by using Silica/ polystyrene lens array [80]. It has been reported that textured ITO with Ag nanoparticle can enhance light output power by 20.2% [81]. Hsiao et al. showed LEE enhancement of 10.5% with syringe-like ZnO nanorod structure [82].

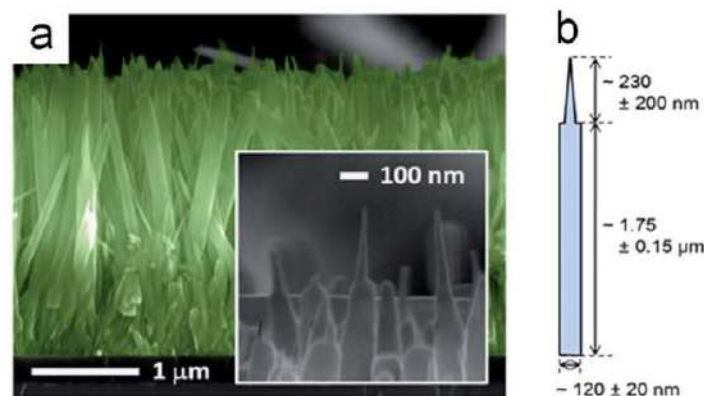


Figure 2.6: (a) SEM image and (b) schematic of a syringe-like ZnO nanorods [82].

2.9.2 Substrate Engineering

In LED devices, a significant amount of light is also scattered downwards into the substrate. Therefore LEE can be further enhanced by substrate engineering and restoring the photons that are scattered in the downward direction.

2.9.2.1 Nanoscaled patterned substrate

The nanopatterned substrate can reduce dislocations and enhance light scattering and thus result in higher LEE (Figure 2.7 (a)-(b)). Cheng et al showed superior LEE performance by introducing hybrid micro-nano PSS [83]. It has also been reported that utilization of PSS, a 44% reduction in the TD densities and a 224% enhancement of IQE factor can be achieved by utilizing PSS [84].

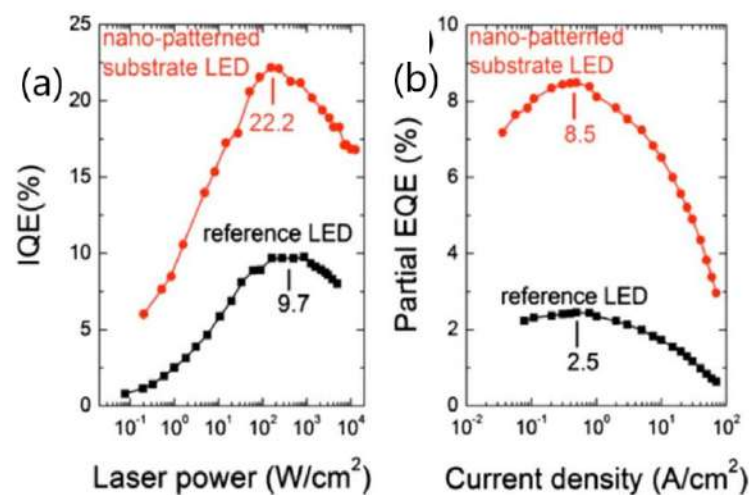


Figure 2.7: (a) IQE and (b) EQE with current density for nanopatterned substrate LEDs and reference LEDs [84].

2.9.3 Surface-plasmon enhanced LEDs

QW-SP coupling can significantly boost the LEE of GaN LED devices as shown in Figure 2.8. If there is a metal-dielectric interface near the QW structure and if there is a close match between the frequencies of electron oscillation in the metal and emitted light, then there can be a strong coupling between QW-SP. It has been reported that significant enhancement of LEE can be possible with efficient QW-SP coupling [74].

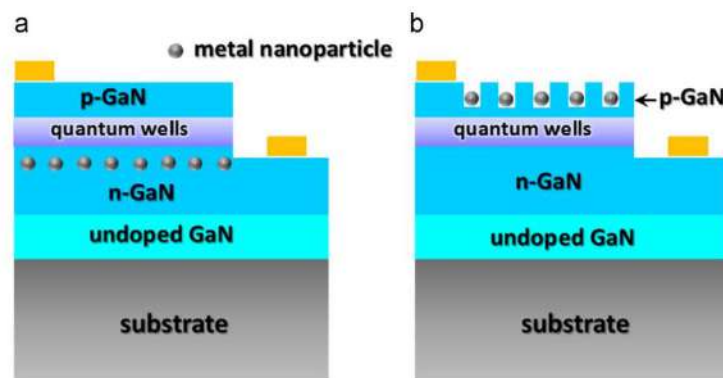


Figure 2.8: LED devices with (a) embedded nanoparticles in n-GaN and (b) nanoparticles in etched p-GaN layer to couple QW-SP [74].

Chapter 3

Simulation Framework, Methodology, and Structural Modeling

This chapter elaborates on the simulation framework and methodology used for evaluating the extraction efficiency of LED devices. Moreover, we also focus on modelling single, nanowire-array based and micro LED structures. Simulation set-up for LEE enhancement is also introduced in the later portion of this chapter. Finally, this chapter deals with the numerical methods used for calculating extraction efficiencies considering the degree of polarization.

3.1 FDTD Simulation

In our study of LEE of nanowire and micro LEDs, we used finite difference time domain (FDTD) based optical simulation. FDTD simulation is a numerical method used to solve Maxwell's electromagnetic field equations. It is extremely helpful for studying how electromagnetic waves propagate through complicated structures. Besides analyzing the electromagnetic wave propagation and emission pattern for our LED structures, we also calculated the extraction efficiencies of our devices using this numerical method.

3.2 Maxwell's Equations and the FDTD Method

FDTD is an extremely popular numerical method to simulate photonic processes, devices and structures. Based on Maxwell's electromagnetic field equations, the FDTD

method is the most basic electromagnetic field solver. In their macroscopic forms, Maxwell's electromagnetic equations are represented as:

$$\nabla \cdot \mathbf{E} = \frac{\rho}{\epsilon} \quad [\text{Gauss's Law}] \quad (3.1)$$

$$\nabla \cdot \mathbf{B} = 0 \quad [\text{Gauss's Law for magnetism}] \quad (3.2)$$

$$\nabla \times \mathbf{E} = -\frac{\partial \mathbf{B}}{\partial t} \quad [\text{Maxwell - Faraday equation}] \quad (3.3)$$

$$\nabla \times \mathbf{B} = \epsilon \left(\mathbf{J} + \mu \frac{\partial \mathbf{E}}{\partial t} \right) \quad [\text{Ampere' Law}] \quad (3.4)$$

Maxwell's four equations play a major role in electromagnetics as they govern the master equation used in the FDTD method to describe and simulate photonic structures such as nanowires, nanowire arrays and planar LED structures in our studies.

Kane S. Yee introduced the FDTD approach in one of his most influential publications [85]. He did this by applying centred finite difference operators to discretized grids in space and time for each electric and magnetic vector field component in Equations 3.3 and 3.4 as shown in Figure 3.1.

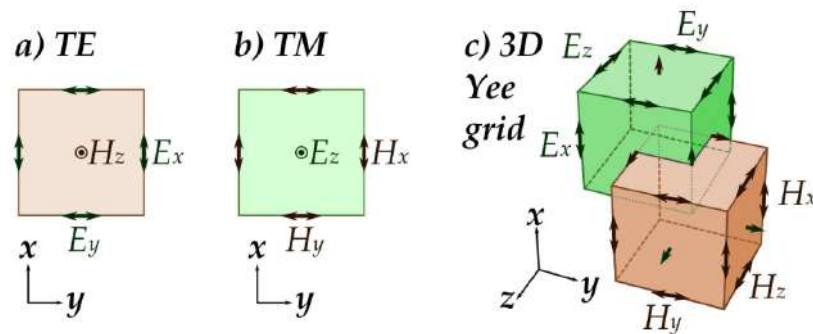


Figure 3.1: Representation of a standard Yee cell used in FDTD method illustrating how electric and magnetic field vectors are distributed [86].

It is quite evident from the above equations that the electric field in time and the magnetic field in space are interconnected. That's why the value of the electric field in time at any point in space depends on its previous value and the numerical curl of the local magnetic field distribution in space. The value of the magnetic field in time at any location in space is similarly influenced by the value of the magnetic field in the past and the numerical curl of the regional distribution of the electric field in space. As a result,

for each grid point in the space under consideration, the coupled electric and magnetic field equations are solved in a time-stepping manner.

This is an iterative process, as shown in Figure 3.2, and the computation doesn't stop until the field values have reached a steady state, decayed to close to zero, or a predetermined threshold value that effectively renders them irrelevant. Because the FDTD method is a time-domain approach, it can simulate a wide frequency range in a single run by utilising Fourier transformations. This method can also work with nonlinear material characteristics and optically active materials for lasing. Each grid cell in the

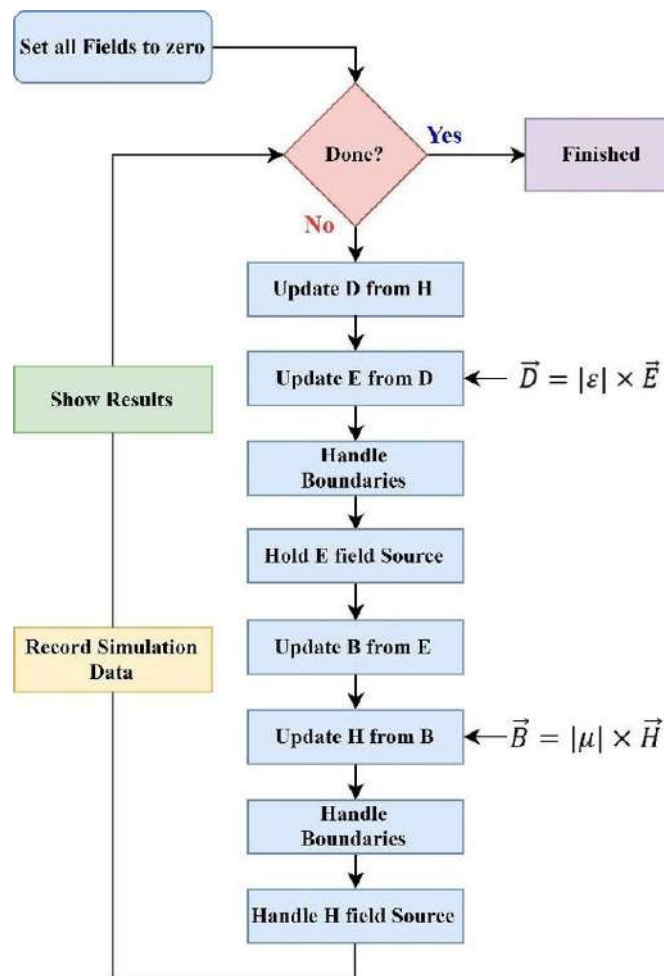


Figure 3.2: Different steps in the FDTD method in the form of a flowchart. [87].

FDTD method is referred to as a Yee cell because it solves Maxwell's equations on a discrete spatial and temporal grid. Each FDTD cell has three electric and three magnetic fields, for six field values. Figure 3.1 shows the distribution of the electric and magnetic field vector components in a typical Cartesian Yee cell used in FDTD. The electric field components create the cube's edges, while the magnetic field components create the cube's faces' normals. By giving the right quantities of permittivity to each electric field component and permeability to each magnetic field component, the inter-

action of the electromagnetic wave with the photonic structure is mapped. A simulation mesh or FDTD volume is produced by mixing several FDTD cells. Most FDTD solution packages define the geometry of the FDTD region and the photonic structures using cartesian or cylindrical coordinate systems. Materials are defined by their optical properties, such as refractive index, dielectric constant, and permeability. Simulations can be run using the FDTD approach in one, two, or three-dimensional spaces. However, as the dimension grows, so do the costs and complexity of computing. In addition, there is a trade-off between computing time and calculation accuracy, which is determined by the spatial resolution (number of grid or mesh points) and the temporal resolution (distance between successive evolution of the fields).

In summary, the basic steps involving FDTD simulations are:

1. Defining the geometry
2. Discretizing the domain
3. Initializing the field values
4. Applying boundary conditions
5. Updating the field values
6. Repeating steps 4 and 5 until convergence or allocated time
7. Analyzing the results

3.3 Modeling LED Structures

3.3.1 Nanowire LED Structures

Our study mainly focused on nanowire-based LED devices due to several advantages over planar micro LEDs as mentioned earlier. A schematic of two different type of nanowire-based nitride LED devices is shown in Figure 3.3 (a)-(b). Like traditional QW LED devices, nanowire LED devices also consist of a p-layer, an n-layer and active quantum well layers. In a radial QW LED structure, the active QW layers are radially sandwiched between p and n-layer (Figure 3.3a). On the contrary, the QW layers form an inner hollow cylindrical structure between p and n-type material in axial QW LED structures. Three different polarizations of the dipole source are shown in Figure 3.3(c), and in this work, we extensively studied the effects of polarization on

LED performance. In our study, we explored the effect of two different dipole polarizations: TE polarization and TM polarization. For TE polarization Electric field intensity vector is perpendicular to the axis of the nanowire cylinder. The E-field intensity vector is always parallel to the cylindrical axis for TM polarisation.

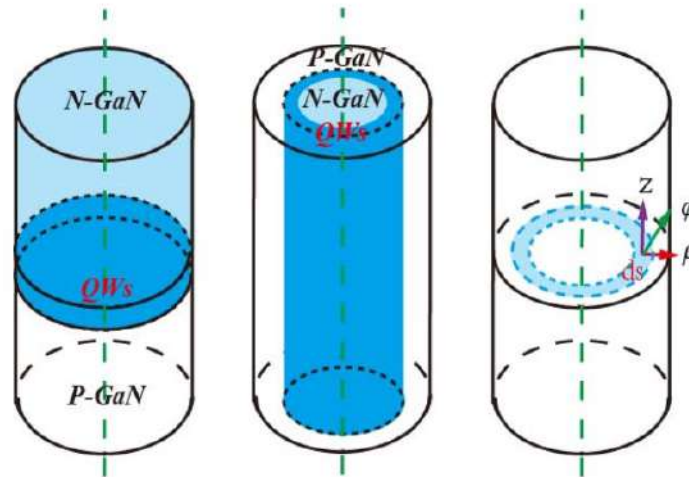


Figure 3.3: Schematic of (a) radial QW and (b) axial QW nanowire-based LED structures, and (c) three different dipole polarizations in a cylindrical nanowire. [11].

Only radial QW nanowire LED structures were explored as they are more popular, and we studied both InGa_N/Ga_N MQW-based LED structures for visible (specifically blue) emission and AlGa_N/AlGa_N MQW based nanowire LED structures operating in the UV-C wavelength range. The longitudinal cross-sections of both of these LED structures are shown in Figure 3.4.

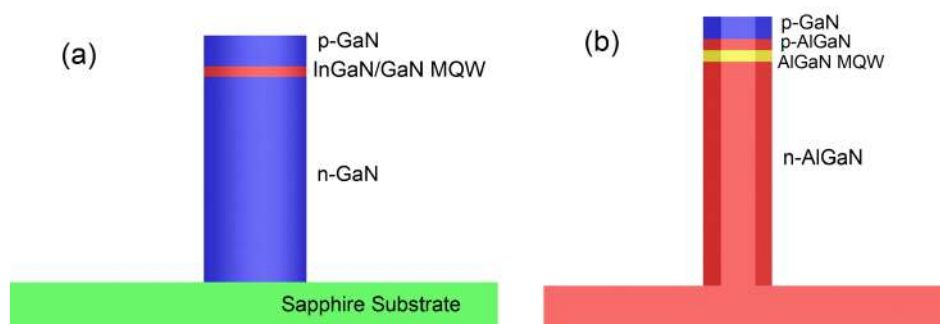


Figure 3.4: Schematic of a longitudinal cross-section of two different types of nanowire LED structures: (a) InGa_N/Ga_N MQW based nanowire LED structure and (b) AlGa_N MQW based nanowire LED structures showing material compositions.

The material composition of both of the nanowire-based LED devices is also shown in Figure 3.4. The refractive index value of each layer is taken from the literature. For InGa_N LED devices, we considered cylindrical structures with circular cross-sections; for AlGa_N LED devices grown on a sapphire substrate, we considered a cylindrical

nanowire structure with a hexagonal cross-section. We evaluated these LED devices' top and side extraction efficiencies for different emission polarizations. We also explored the effect of nanowire dimensions and distance between the adjacent nanowires on extraction characteristics. Furthermore, we proposed several methods for improving the overall efficiency of these emitters.

3.3.2 Planar Micro LED Devices

Besides nanowire-based LEDs, we also studied extraction characteristics of planar InGaN and AlGaIn-based micro-LED devices. The material composition of the micro LED device was kept identical to that of nanowire-based LED devices. A schematic of the micro LED structure with a width of 5 μm is shown in Figure 3.5.

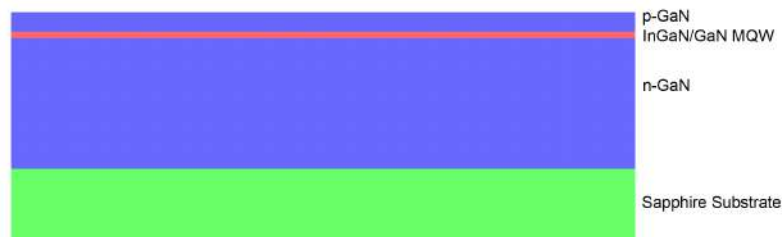


Figure 3.5: Schematic of cross-section of InGaN/GaN MQW based planar micro LED devices showing material compositions.

3.4 Simulation Setup

3.4.1 Single Nanowire LED Structure

In order to calculate LEE values and investigate the emission pattern, we employed 3D FDTD-based optical simulations. For calculating the extraction efficiencies of the single nanowire, we first defined the geometry and then set the material parameters. We then placed a dipole source in the active layer to simulate the emission from these devices. The wavelength and polarization of the dipole source were set according to the simulation requirements. For simulating a single nanowire structure, we used PML (Perfectly Matched Layer)- which acts like a perfect absorbing layer- boundary conditions in all directions. A collection of planar power monitors were then placed to calculate the power through these planes. A total of six planar power monitors are placed inside the nanowire surrounding the dipole source to measure the source dipole power/

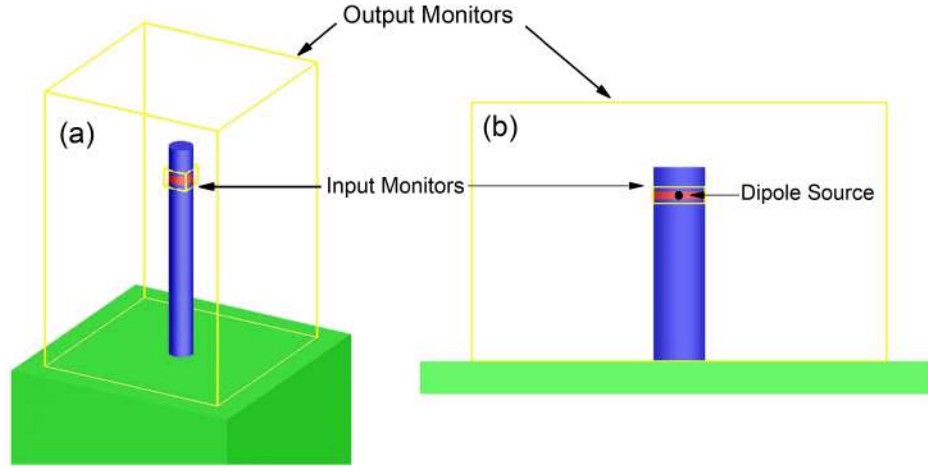


Figure 3.6: Simulation setup for LEE calculation of nanowire-based LED devices. (a) Perspective view showing nanowire structure, dipole source, simulation region, boundary layers, and output power monitors. (b) Planar cross-sectional view of the simulation setup showing input power monitors inside the nanowire for measuring the dipole source power.

input power. The power of each of the monitors was added to calculate the overall input power as shown in Equation 3.6. Similarly, a collection of five planar power monitors are placed externally surrounding the nanowire structure as shown in Figure 3.6. The four power monitors surrounding the nanowire structures have been used to measure the power transmitted through the sideways direction, P_{Side} . A power monitor on top of the nanowire structure measured the power that could be extracted from the top side, P_{Top} . Using Equations 3.5-3.11, we finally calculated the side, top and total extraction efficiencies defined by LEE_{Top} , LEE_{Side} , and LEE_{Total} respectively. All the relevant equations for LEE calculation follow:

$$P_{in} = P_{in1} + P_{in2} + P_{in3} + P_{in4} + P_{in5} + P_{in6} \quad (3.5)$$

$$P_{out(Top)} = P_{Top} \quad (3.6)$$

$$P_{out(Side)} = P_{Side1} + P_{Side2} + P_{Side3} + P_{Side4} \quad (3.7)$$

$$P_{out(Total)} = P_{out(Top)} + P_{out(Side)} \quad (3.8)$$

$$LEE_{Top} = \frac{P_{out(Top)}}{P_{in}} \quad (3.9)$$

$$LEE_{Side} = \frac{P_{out(Side)}}{P_{in}} \quad (3.10)$$

$$LEE_{Total} = LEE_{Top} + LEE_{Side} = \frac{P_{out(Total)}}{P_{in}} \quad (3.11)$$

Moreover, top, side and total light extraction efficiencies for TM polarization are denoted as $LEE_{TM(Top)}$, $LEE_{TM(Side)}$, and $LEE_{TM(Total)}$ respectively. Similar notations

have been used throughout this work for TE polarization also.

3.4.2 Periodic Nanowire Array Structure

In addition to studying emissions from single nanowires, we explored periodic nanowire array LEDs. In a practical nanowire-based LED device as shown in Figure 3.7, there will be an array of multiple nanowires arranged in a periodic configuration where each nanowire would be used as an individual emitter.

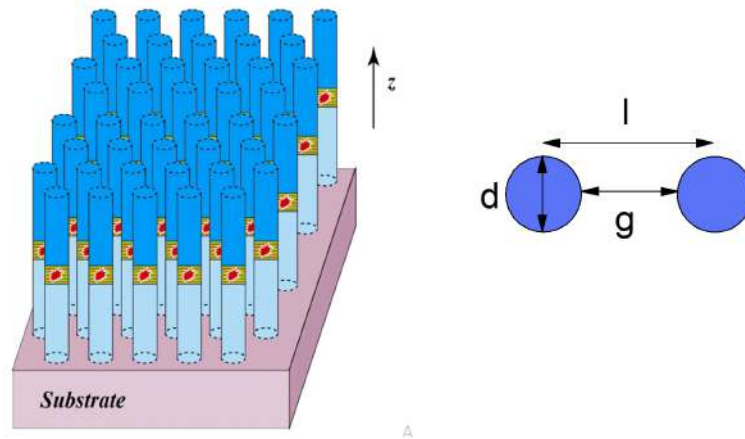


Figure 3.7: A schematic representation of a nanowire-array based LED devices [11].

To simulate a periodic nanowire array, we only simulated a unit cell. The boundary condition was set as a periodic boundary condition for the four boundaries surrounding the unit cell as shown in Figure 3.8. Moreover, PML boundary condition was set at the top and bottom of the unit cell (Figure 3.8). Moreover, we considered a square periodic arrangement. The geometry of the FDTD simulation region was selected according to the array periodicity. In our results, we reported extraction characteristics in terms of the gap between the two neighbouring nanowires, where the gap, g is defined as:

$$g = l - d \quad (3.12)$$

where l describes the distance between the centres of adjacent nanowires, and the nanowire diameter is defined as d .

We only calculated the top extraction for periodic nanowire array arrangement and hence placed a top power monitor to calculate the power that can be extracted from the top side as shown in Figure 3.8. Besides, we calculated the source power in the same way as mentioned before.

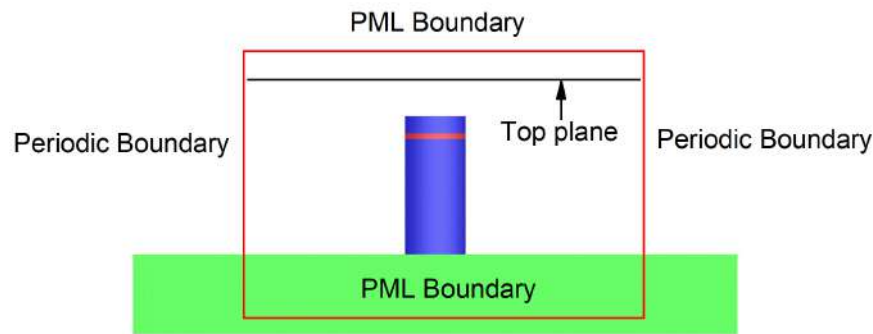


Figure 3.8: A unit cell for simulating nanowire periodic arrays indicating boundary conditions and top extraction plane.

3.4.3 2D Simulations for Planar Micro LED Structures

In order to calculate the extraction efficiencies for micro-LED devices, we performed 2D FDTD simulations. We simulated micro LED devices with diameters up to 50 μm , and to reduce the computational complexity, we only performed 2D simulations. Furthermore, we observed similar characteristics for our 3D simulations and decided that 2D simulation would give us a general idea about extraction characteristics. In our simulation, four linear power monitors inside the active region were used to measure the dipole source power. And one top and two side linear monitors were used to measure the top and side extracted powers as shown in Figure 3.9.

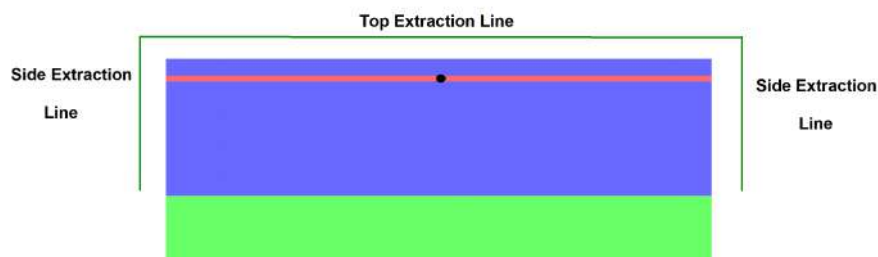


Figure 3.9: A schematic of a micro LED device with top and side extraction lines for calculating top and side extraction.

3.4.4 Structure with inclined reflectors

In Section 7, we analyzed two methods for LED LEE enhancement, and one of the methods was the introduction of inclined side reflectors, as shown in Figure 3.10.

In this research work, we performed 2D simulations for analyzing the effect of inclined reflectors on overall extraction characteristics in order to reduce computational time and complexity. However, we validated our results with 3D simulations and found 2D sim-

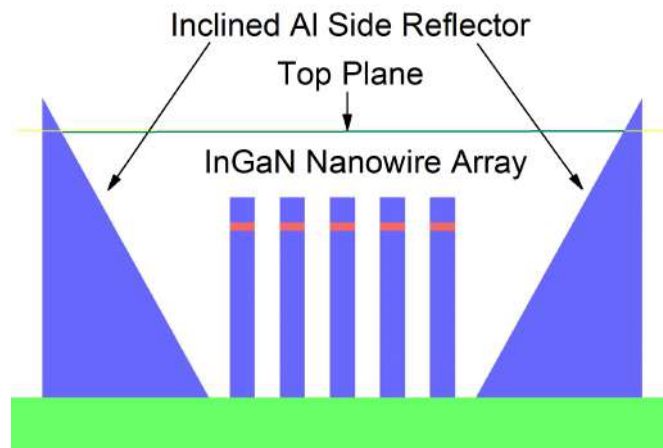


Figure 3.10: A schematic showing a periodic nanowire array arrangement with inclined sidewall reflector for enhancing the top extraction.

ulation to be a good approximation. We only considered a 1D periodic arrangement of five nanowires and placed two inclined Al-side reflectors on both sides. PML boundary condition was set at all the boundaries. Finally, a top linear power monitor was placed to calculate the top extraction. To analyze the impact of inclined side reflectors, we then eliminated the side reflectors and calculated the extraction without the side reflectors and calculated the LEE enhancement.

3.5 Degree of Polarization and LEE calculation using DOP

Calculating LEE considering DOP is one of the major contributions of this study. In order to incorporate DOP in LEE calculation, we used two simple methods: The weighted Average method and Polarization Angle Method.

3.5.1 Weighted Average Method

In the weighted average method, we initially calculated side, top and total extraction efficiencies for both TE and TM polarizations. From the reported DOP value, we calculated the ratio of TE and TM polarization intensities. This ratio is defined as m . This ratio was then used as the weight for calculating the LEE considering DOP. All the

necessary equations for calculating LEE considering the DOP value are as follows:

$$\begin{aligned}
 DOP &= \frac{I_{TE} - I_{TM}}{I_{TE} + I_{TM}} \\
 (I_{TE} + I_{TM}) DOP &= I_{TE} - I_{TM} \\
 I_{TE}(DOP - 1) &= -I_{TM}(1 + DOP) \\
 I_{TE}(1 - DOP) &= I_{TM}(1 + DOP) \\
 \frac{I_{TE}}{I_{TM}} &= \frac{1 + DOP}{1 - DOP} \\
 \text{Let, } \frac{I_{TE}}{I_{TM}} &= \frac{1 + DOP}{1 - DOP} = m
 \end{aligned} \tag{3.13}$$

The overall extraction efficiency considering DOP , $LEE_{overall}$ is defined as:

$$\begin{aligned}
 LEE_{overall} &= \frac{P_{out}}{P_{in}} \\
 &= \frac{P_{TM(out)} + P_{TE(out)}}{P_{in}} \\
 &= \frac{P_{TM(out)}}{P_{in}} + \frac{P_{TE(out)}}{P_{in}}
 \end{aligned} \tag{3.14}$$

From Equation 3.13 we get,

$$\frac{I_{TE}}{I_{TM}} = \frac{P_{TE(in)}}{P_{TM(in)}} = m \tag{3.15}$$

$$P_{TE(in)} = m P_{TM(in)} \tag{3.15}$$

$$P_{TM(in)} = \frac{1}{m} P_{TE(in)} \tag{3.16}$$

Now, from Equations 3.14, 3.15 and 3.16, we can write the following:

$$\begin{aligned}
 LEE_{overall} &= \frac{P_{TM(out)}}{P_{TM(in)} + P_{TE(in)}} + \frac{P_{TE(out)}}{P_{TM(in)} + P_{TE(in)}} \\
 &= \frac{P_{TM(out)}}{P_{TM(in)} + m P_{TM(in)}} + \frac{P_{TE(out)}}{\frac{1}{m} P_{TE(in)} + P_{TE(in)}} \\
 &= \frac{P_{TM(out)}}{(1 + m) P_{TM(in)}} + \frac{P_{TE(out)}}{\left(1 + \frac{1}{m}\right) P_{TE(in)}} \\
 &= \frac{P_{TM(out)}}{(1 + m) P_{TM(in)}} + \frac{m P_{TE(out)}}{(1 + m) P_{TE(in)}} \\
 &= \frac{1}{1 + m} LEE_{TM} + \frac{m}{1 + m} LEE_{TE}
 \end{aligned}$$

$$LEE_{overall} = \frac{m}{1+m} LEE_{TE} + \frac{1}{1+m} LEE_{TM} \quad (3.17)$$

Here, we define TE and TM polarization intensities as I_{TE} and I_{TM} , output power for TE and TM polarizations as $P_{TM(out)}$ and $P_{TE(out)}$. Moreover, extraction efficiencies for TM and TE polarizations are defined as LEE_{TM} and LEE_{TE} .

3.5.2 Polarization Angle Method

Besides Weighted Average Method, we also proposed another method for LEE calculation taking DOP into consideration. In this method, we calculated the LEE values without the LEE values for TE and TM polarizations. Just like the previous method, the ratio of intensities for TE and TM polarization was calculated from the reported DOP value (Equation 3.13). Then using this ratio, the polarization angle (θ) of the dipole source was set accordingly as shown in Equation 3.18.

$$\begin{aligned} \text{Let, } \frac{I_{TE}}{I_{TM}} &= m \\ \tan \theta &= \frac{1}{m} \\ \theta &= \tan^{-1} \left(\frac{1}{m} \right) \end{aligned} \quad (3.18)$$

Here, all the symbols have their usual meanings. A schematic showing the dipole polarization angle with respect to TE and TM polarization is shown in Figure 3.11.

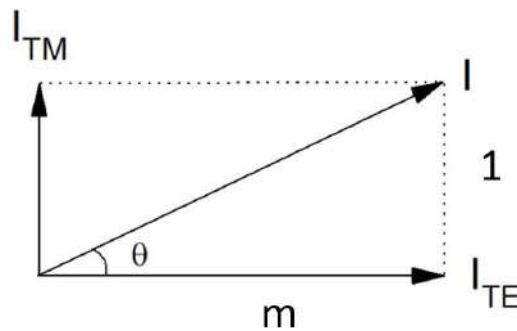


Figure 3.11: A schematic showing the polarization angle of the dipole source with respect to TE and TM polarization.

LEE value calculated for this dipole polarization angle is the final LEE value considering DOP. The results obtained from both of these methods were the same and this also verified the validity of the weighted average method. The advantage of the polarization

angle method is that we can calculate the LEE values from a single simulation run and we don't need LEE values for TE and TM polarizations. However, in the weighted average method, we do require LEE values calculated for both polarizations. As the LEE value is just the weighted average of LEE values calculated for TE and TM polarizations, we need to understand the extraction characteristics for both polarizations to explain the overall extraction characteristics. So, to explain the extraction characteristics, it is much better to know the extraction characteristics for both polarization components. Hence, in our study, we used the weighted average method for calculating extraction values.

Chapter 4

Impact of Nature of Polarization and Nanowire Dimension on LEE

Emission polarization and the dimension of the nanowires play a crucial role in the overall extraction characteristics of nanowire-based and micro LED devices. In this chapter, we elaborate on the impact of polarization on the side and top extraction of nanowire LED devices and also explain the characteristics in terms of waveguiding nature of these devices. Also, the impact of the nanowire dimension on the overall extraction characteristics is studied in detail in this chapter.

4.1 LEE of InGaN-Based LEDs

4.1.1 Structural Composition of InGaN nanowire LED

Initially, we examined the extraction efficiency of a single nanowire InGaN LEDs operating in the visible wavelength and initially, only considered the emission wavelength of 400 nm. We explored the effect of nanowire dimension and emission polarization on top, side and total extraction efficiencies incorporating the effects of the several waveguiding modes. We selected a nanowire LED structure composed of a 2 μm thick n-GaN layer, 50 nm thick InGaN/GaN MQW region, and 150 nm thick p-GaN layer assumed to be grown on the sapphire substrate as shown in 3.4(a). The real and imaginary parts of the complex refractive index value for these materials were set according to the values reported in the literature [24]. We placed a dipole source in the active region of the nanowire structure and set the emission wavelength at 400 nm. Different dipole polarizations (TE and TM) are used to simulate different polarization natures of emis-

sion. We calculated the top and side extraction efficiencies for different polarizations and nanowire diameters for 400 nm emission wavelength.

4.1.2 Side and Top Extraction for TE and TM Polarizations

For both TE and TM polarizations, the nanowire diameter d was varied from 50 nm to 400 nm. It is quite evident from Figure 4.1 (b) and (d) that, for a single nanowire LED structure, side extraction is higher compared to top extraction for both polarizations. However, top extraction efficiency as high as 30% can be obtained for TE polarization, whereas the highest extraction efficiency for TM polarization is less than 15%. This is due to the relatively higher side extraction nature of the TM polarization, as evidenced by the electric field distribution for TM polarization. For TE polarization, we have observed relatively higher top extraction efficiency compared to TM polarization. It is also verified by the E-field distribution pattern as shown in Figure 4.1(a) and (c). We have also observed various distinct peaks in the efficiency characteristics, which can be explained by the effect of several wave-guiding modes, which will be elucidated in detail.

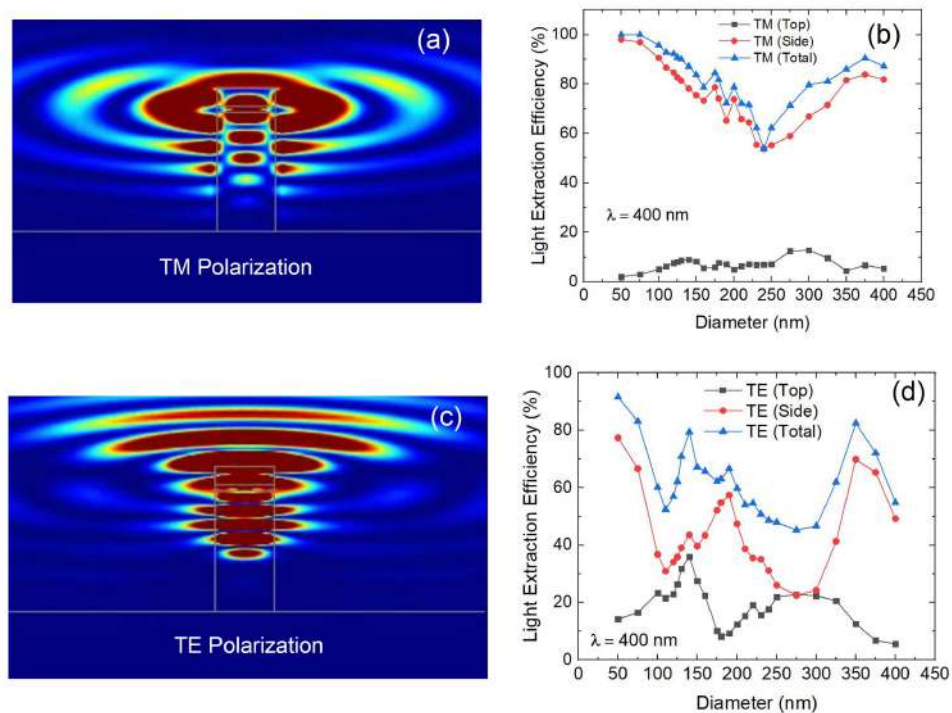


Figure 4.1: Emission characteristics for TM and TE polarization. (a) Electric field distribution and (b) top, side and total extraction efficiencies for TM polarization. (c) Electric field distribution and (d) top, side and total extraction efficiencies for TE polarization.

Especially for TM polarization, the side extraction value is much higher compared to top extraction and thus, total extraction efficiency is mainly governed by the side extraction (Figure 4.1(b)). For a nanowire diameter less than 100 nm, total extraction due to high side extraction is almost 100% and top extraction is almost negligible. However, as we increase the nanowire diameter, the total and top extraction exhibit a downward trend and beyond the nanowire diameter of 200 nm, top and total extraction once again increase with nanowire dimension. The increasing trend of side extraction with nanowire dimension is also evident from the E-field pattern. We know that modal characteristics become less prominent as we increase the dimension and we suspect that less power is coupled to the guided modes and hence enhancing the overall side extraction. We also observe more electric field confinement inside the nanowire and relatively higher.

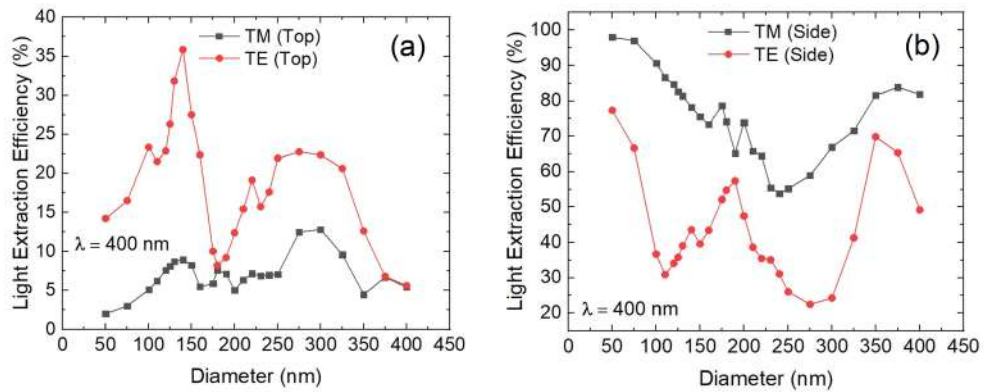


Figure 4.2: . Comparison between (a) top and (b) side extraction efficiency for TE and TM polarization

For TE polarization, we don't observe any particular trend rather we observe clear oscillations in the efficiency curve (Figure 4.1(d)). We observe several peaks in the top extraction related to several waveguiding modes. As mentioned earlier, the top extraction efficiency is also quite high compared to TM polarization (Figure 4.2). It is due to the field pattern for TE polarization and relatively stronger coupling to the guided modes. For a nanowire diameter of 140 nm, we observe top extraction efficiency of almost 30% and top and side extraction is almost similar for the nanowire diameter of 275 nm. As the emission characteristic of InGaN LED is mostly TE polarized, we observe relatively higher top extraction efficiency compared to AlGaN UV LED where the emission is mostly TM polarized [47]. So, polarization nature plays a significant role in the side, top and total extraction and engineering polarization nature can enhance the extraction profile.

Table 4.1: For a dielectric cylinder with $\epsilon = 6.25$ in air, the cutoff values for several lowest order modes [88]

| Mode | a/λ | Mode | a/λ |
|--------------------|-------------|--------------------|-------------|
| HE_{11} | 0 | TE_{01}, TM_{01} | 0.166 |
| HE_{21} | 0.229 | EH_{11}, HE_{12} | 0.265 |
| HE_{31} | 0.328 | EH_{21} | 0.355 |
| TE_{02}, TM_{02} | 0.382 | HE_{41} | 0.418 |
| HE_{22} | 0.428 | EH_{31} | 0.441 |

4.1.3 Effect of Waveguiding Modes on Extraction Characteristics

In this section, we will elucidate the influence of waveguiding modes on the top extraction efficiency and how it influences side and total extraction. For a dielectric cylinder with epsilon = 6.25, the cut-off values for several lowest-order modes are shown in Table 4.1 and the Electric field intensity distribution of the several lowest-order guiding modes are shown in Figure 4.3.

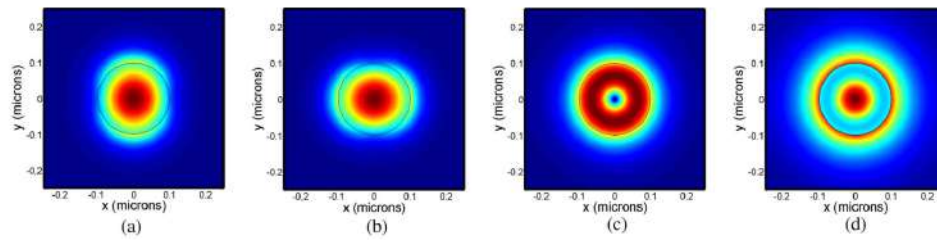


Figure 4.3: Electric field intensity distribution of four lowest order guiding modes for a nanowire with a diameter of 200 nm. [88]

From Figure 4.4, we observe the presence of multiple peaks in the top extraction efficiency and they correspond to several lowest-order guided modes. It has been reported that LEE reaches local maximum values just before the mode cut-off radius and LEE gradually decreases after the mode cut-off radius [88]. The lowest order mode HE_{11} doesn't have a cutoff radius however as we increase the diameter up to 140 nm, we observe that the top extraction efficiency keeps on increasing with dimension. The reason behind this is that as we keep on increasing the diameter the modes get more confined inside the nanowire resulting in much greater waveguiding characteristics and enhanced top extraction. Furthermore, it has been shown that for a particular mode, the reflectivity from the end facets also increases with the nanowire dimension. For smaller diameters, the mode is poorly confined and the field extends far beyond the nanowire surface hence we observe lower top extraction. Moreover, in our simulation, we also observe that this peak occurs just before the cut-off radius for TE_{01} and TM_{01} mode as mentioned in Table 4.1 and putting $\lambda = 400$ nm. Similarly, the other peaks at 175 nm, 220 nm and 275

nm correspond to the HE_{21} , EH_{11} and HE_{31} modes respectively and we once again observe the peaks occurring just before the mode cut-off radius (Figure 4.4).

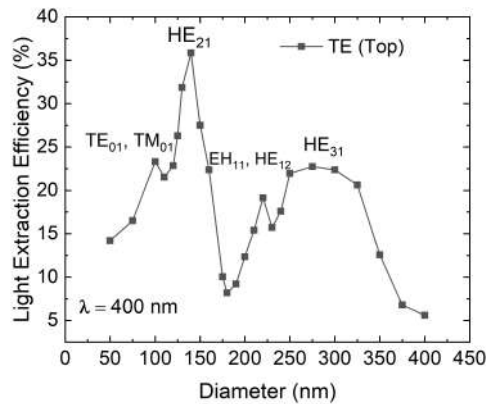


Figure 4.4: Top extraction efficiency for TE polarization.

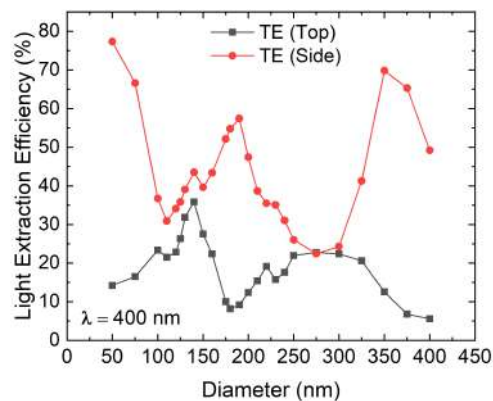


Figure 4.5: Comparison between top and side extraction efficiency for TE polarization.

We can also relate the side extraction for TE polarization with the waveguiding characteristics. As shown in Figure 4.5, before the first mode cut-off radius, the top extraction keeps on decreasing and on the other hand, the side extraction improves with dimension. Similarly, this opposite trend between side and top extraction is also prominent after the mode cut-off radius. As the top extraction is going down, we observe an upward trend for the side extraction. And the total extraction is only the summation of these two extractions. Hence side and top extraction characteristics can be explained in terms of waveguiding modal characteristics.

4.2 LEE of AlGaN LEDs Operating at DUV

AlGaN materials-based UV LEDs operating at deep UV or UV-C Wavelengths (200-280 nm) have garnered significant attention due to numerous potential applications in

disinfection, purification, and sterilization of water and air. Our AlGaIn-based UV LED is assumed to be grown on a sapphire substrate and is composed of 2 μm thick n-AlGaIn layer, 50 nm thick AlGaIn MQW layer, 50 nm thick p-AlGaIn layer and finally 100 nm thick p-GaN top contact layer (Figure 3.4(b)). The (n,k) parameters for these materials are taken from the literature [41]. Moreover, in order to simulate the realistic case, we considered the hexagonal cross-section of our nanorod LED structure, and we examined the extraction characteristics at UV-C (200-280 nm) and initially limited our analysis to only 250 nm wavelength.

4.2.1 Side and Top Extraction Efficiencies for TE and TM Polarizations

Just like InGaIn LED, we extensively studied the top and side extraction efficiency of AlGaIn nanowire UV-LEDs for both TE and TM polarizations. Firstly, we noticed several peaks in the extraction efficiency characteristics related to several modes in the nanowire (Figure 4.6). The lower top extraction efficiency is due to the presence of a highly absorbing p-GaN top contact layer. The high absorption coefficient of the p-GaN layer at UV-C severely limits top extraction efficiency for LEDs and hence the enhancement of extraction efficiency of UV-C LED is a topic of ongoing research.

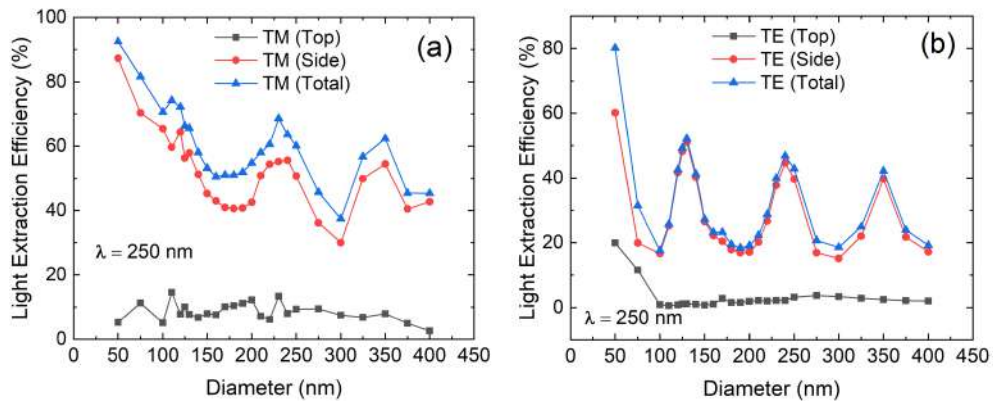


Figure 4.6: Top, side and total extraction efficiencies of UV-C AlGaIn nanowire LEDs for (a) TM polarization and (b) TE polarization.

For the case of TE polarization, as usual for small nanowire diameter, LEE is quite high (almost 90%) due to weak mode confinement and weak coupling to the guided modes. As predicted, side extraction is significantly higher compared to top extraction. Maximum side and top extraction efficiencies are 60% and 19% respectively. We also notice distinct peaks in the side and total extraction characteristics. Due to almost insignificant top extraction efficiency for all the diameters larger than 100 nm, the total extraction is

almost equal to side extraction efficiency (Figure 4.6). The peaks in the side and total extraction are observed at diameters 130 nm, 240 nm and 350 nm respectively which are related to the cut-off radius of several lower-order waveguiding modes as described earlier in this section. Furthermore, we notice that the side and total extraction efficiencies at these peaks are quite similar in values and the side extraction efficiency value is in the range of 39-52%. The Electric field pattern for two diameters in 130 nm (peak) and 190 nm (trough) are shown in Figure 4.7 and these figures can better elucidate the reasons behind high and low extraction efficiencies.

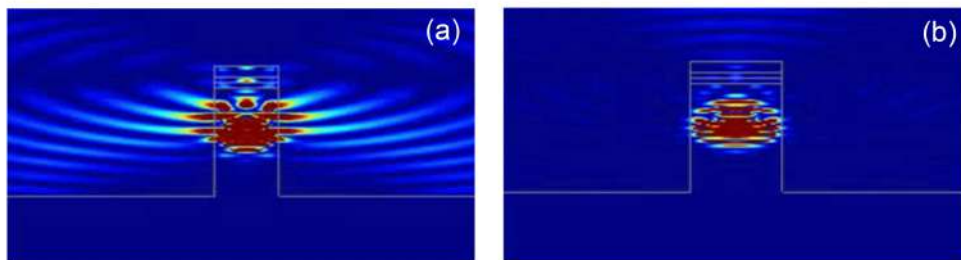


Figure 4.7: E-field pattern showing superior side and total extraction efficiencies for specific diameter. Electric field distribution for TE polarization for diameter (a) 130 nm and (b) 190 nm.

We observe from Figure 4.7 (a) and (b) that, for a nanowire diameter of 130 nm after the initial emission, guided modes are weakly confined within the nanowire and hence leak away through the sideways. Hence the side and total efficiency are quite high for a diameter of 130 nm. On the contrary, for a nanowire diameter of 190 nm, we observe that the guided modes are strongly confined inside the nanowire and hence we observe a dip in the side and total extraction. So, as can be observed in Figure 4.8(b), side extraction actually oscillates in the range of 15-52%.

Similarly, we also focused on the extraction characteristics for TE polarization as shown in Figure 4.6(b). The extraction efficiency is quite high at smaller diameters as expected. Side extraction is once again significantly higher compared to top extraction. Top extraction is relatively higher than TM polarization, which is quite intuitive due to the emission pattern for TE polarization. However, the top extraction efficiency is still quite low due to higher absorption in the p-GaN layer. The maximum value of side and top extraction efficiency is 87% and 15%, respectively. Moreover, the peaks are located at the same diameters as in the case of TE polarization.

4.2.2 Comparison of Extraction Efficiencies between TE and TM polarizations

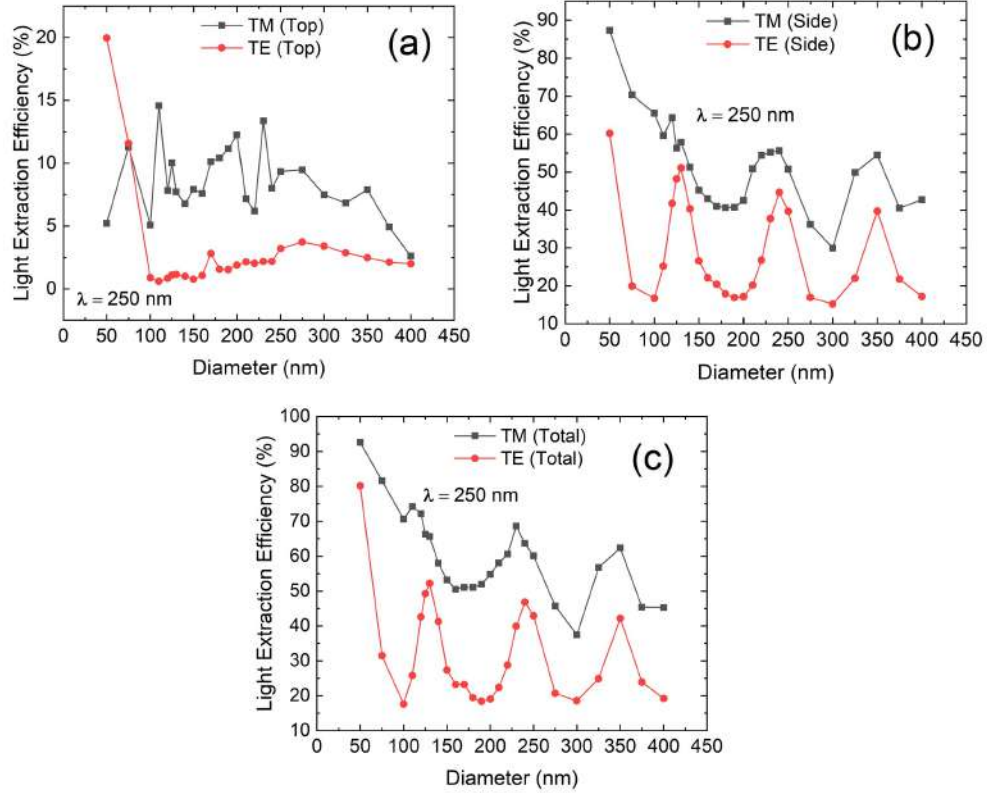


Figure 4.8: (a) Top, (b) side and (c) total extraction efficiency for both TE and TM polarizations.

Here, we will compare the extraction characteristics in more detail as shown in Figure 4.8(a)-(c). A key finding is that for almost all the diameters, side and top extraction are higher for TM polarization compared to TE polarization. Due to the field pattern of the TE-polarized dipole source, absorption in the top p-GaN contact layer is relatively higher. However for nanowire diameter = 50 nm, top extraction for TE polarization is quite high but with increasing nanowire diameter this extraction decreases significantly and for nanowire diameter greater than 100 nm, the top extraction for TE polarization is almost nonexistent. As expected, side extraction for TM polarization is higher than TE polarization due to their field patterns. The peaks are located in the same positions for both TE and TM polarizations. And the total extraction is significantly higher for TM polarization, as shown in Figure 4.8(c).

4.2.3 LEE of InGaN Micro LEDs

We also calculated the extraction efficiency of micro-LED devices for different optical polarizations. The material composition of the InGaN micro-LED devices was set identical to that of nanowire-based LED devices.

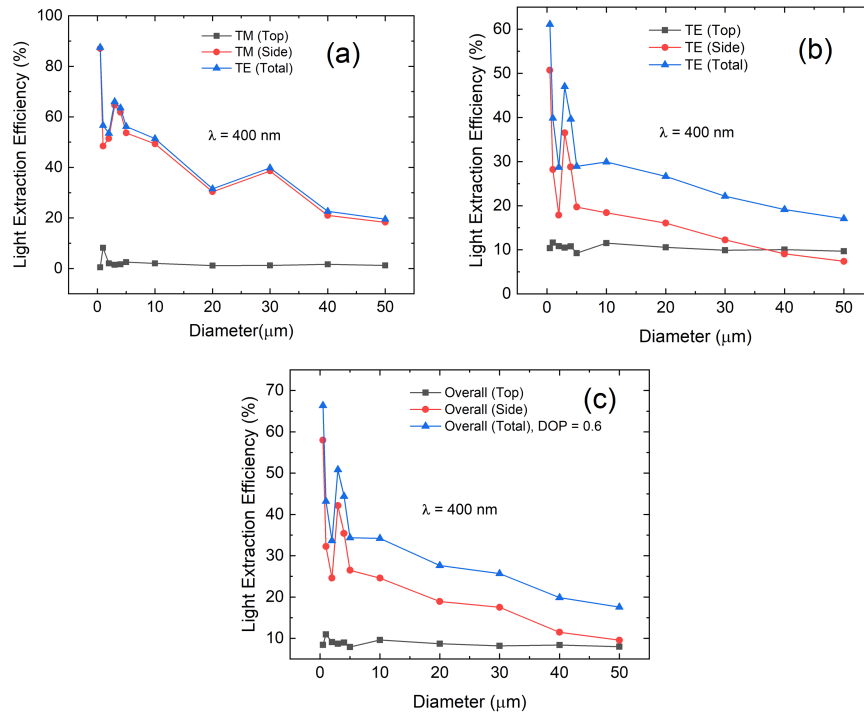


Figure 4.9: Top, side and Total extraction efficiencies of micro-LED devices for (a) TM polarization, (b) TE polarization.

To reduce computational time and complexity, we only performed 2D simulations and found that the results exhibited similarities with the 3D simulations. Furthermore, we only considered the 2D cross-section of circular micro-LED devices. We studied extraction characteristics for micro LEDs with diameters from $0.5 \mu\text{m}$ up to $50 \mu\text{m}$ as shown in Figure 4.9 (a)-(c). We only placed a single dipole source in the middle of the active region, which gave us a basic idea about the general extraction trend with device size. However, in order to more accurately calculate the extraction characteristics, a more detailed simulation with many more dipole sources placed throughout the active region is necessary. From Figure 4.9, we observe a decreasing trend of the LEE with device size for a single dipole source placed at the centre of the active region. Furthermore, side extraction is significantly higher than top extraction for TE and TM polarizations. The maximum top extraction for TM polarization and TE polarization are found to be 8%, and 12%, respectively. The top extraction exhibits lower variability with dimension and remains within a narrow range. However, side extraction demonstrates higher vari-

ability with a decreasing trend with device dimension. It is due to the higher material absorption in the device and substrate while the light escapes through the sides. For a single dipole source placed in the middle, side extraction falls even lower than the top extraction for diameter = 40 μm .

Chapter 5

LEE Calculation Using Degree of Polarization

The light extraction efficiency plays a key role in the overall extraction efficiency of LEDs and LEE depends on the optical polarization nature of the emission. Thus calculating the LEE and understanding the effect of optical polarization nature is very important. In the literature, the LEE of nanowire LEDs is calculated using optical simulations for different optical polarizations (TE or TM). However, in reality, the polarization of the emitted light from these light sources is not purely TE or TM but rather a mixture of both and is denoted by the degree of polarization (DOP). In this section, we will investigate the LEE of nanowire-based LEDs considering the actual optical polarizations denoted by DOP reported in the literature.

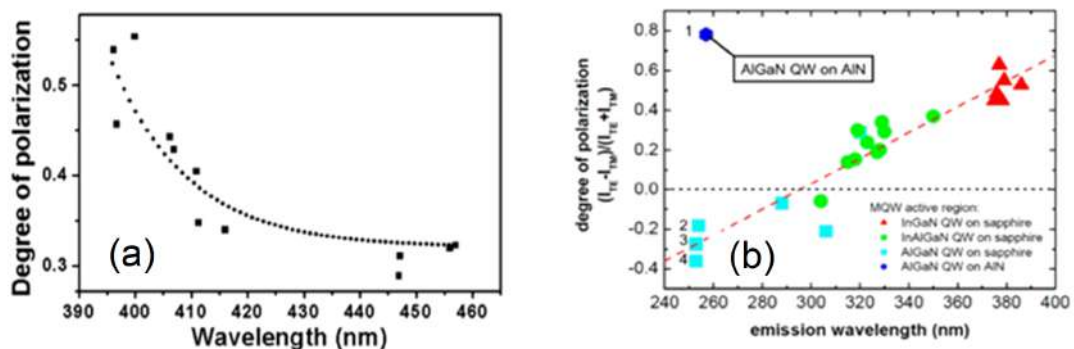


Figure 5.1: Degree of Polarization (DOP) with emission wavelength for (a) InGaN-based LED operating in the wavelength range of 390-460 nm and (b) different group III-Nitride LEDs. [47, 89]

5.1 LEE of InGaN LEDs Considering DOP

Now, we will focus on InGaN/GaN MQW-based LEDs operating in the visible wavelength mainly near the blue region. Unlike for AlGaIn LED, the DOP of InGaN/GaN MQW LEDs is positive which exhibits the TE dominant polarization nature of emission. From Figure. 5.1(a), we observe that the DOP decreases with an emission wavelength in the visible region, and Figure 5.1(b) also reiterates the dominant TE polarization nature of InGaN-based LEDs.

Table 5.1: DOP and the ratio of TE and TM polarization intensities for several emission wavelengths for InGaN-based LED devices [47].

| Wavelength (nm) | DOP | I_{TE}/I_{TM} |
|-----------------|-------|-----------------|
| 400 | 0.6 | 4 |
| 410 | 0.41 | 2.389831 |
| 415 | 0.34 | 2.030303 |
| 447 | 0.31 | 1.898551 |
| 457 | 0.325 | 1.962963 |

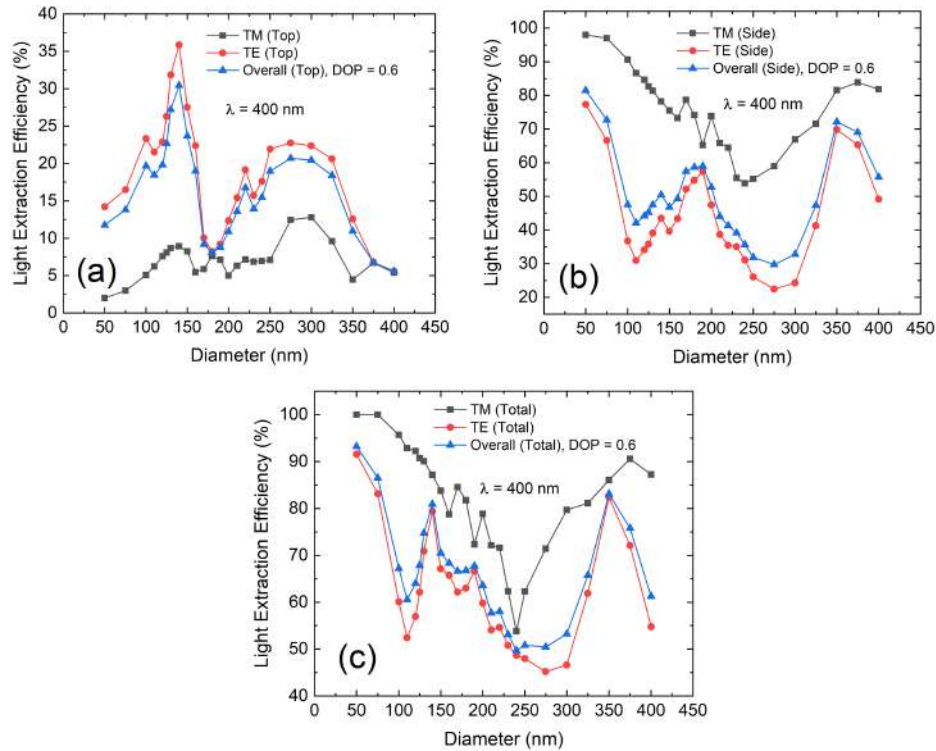


Figure 5.2: Calculation of LEE of InGaN nanowire LED using DOP values. (a) Top, (b) side, and (c) total extraction for DOP = 0.6 at a wavelength of 400 nm.

We initially investigated for emission wavelength, λ at 400 nm. At 400 nm, DOP = 0.6 which results in TE/TM intensity ratio of 4. It suggests that the TE polarization

is significantly dominant and the extraction characteristics will largely be dictated by those obtained for TE polarization. From Figure 5.2(a)-(c), we see that the extraction curves almost match those for TE polarization.

The top extraction is higher for TM polarization due to the radiation pattern and very small absorption loss in the GaN layer at visible wavelength. Hence, top extraction is relatively higher for InGaN-based LEDs. However, the top extraction efficiency is reduced slightly due to the lower extraction of the TE polarization. The maximum top extraction is achieved at a diameter of 140 nm, and the maximum extraction reduces from 36% to 30% after considering the polarization nature. On the other hand, side extraction and overall extraction are relatively lower due to lower side and total extraction for TE polarization as shown in Figure. 5.2(b)-(c). The maximum side extraction is 81% for a nanowire diameter of 50 nm, which is higher than that for TE polarization but significantly less than that for TM polarization. Moreover, the total extraction curve almost resembles that of TE polarization.

5.1.1 DOP Variation with Wavelength

Now, we will study the effect of DOP with the emission wavelength on extraction characteristics. From Figure 5.1(a), we notice the variation of DOP with wavelength and a trend of decreasing DOP with wavelength. We will consider the two extreme cases in the 400-460 nm wavelength range. The DOP value reduces from 0.6 to 0.325 as the emission wavelength is increased from 400 to 457 nm. The extraction characteristics at these two wavelengths are shown in Figure 5.3(a)-(g). Because of the relatively lower DOP value, the TE nature becomes less dominant, and the contribution from TM polarization increases, which also modifies the overall extraction characteristics as shown in the Figures. From Figure 5.3(c) we notice that there is a right shift of the peak and a significant reduction in the maximum top extraction. This is mostly due to the lower DOP value. When the DOP value decreases, then the weight for TM polarization increases (Equation 3.17). We know that the top extraction for TM polarization is relatively smaller. Hence, the higher weight for TM polarization drags the overall top extraction at 457 nm. The peak top extraction reduces from 30% to 23% as the emission wavelength shifts from 400 nm to 457 nm. Another key finding is that the maximum top extraction is obtained for a nanowire diameter of 190 nm at 457 nm as opposed to 140 nm at the wavelength of 400 nm. A completely opposite scenario can be seen for both side and total extractions. The peak for both side and top extractions shifts to a higher wavelength (Figure 5.3(f) and (g)) which is the case for top extraction also.

However, the side and total extraction actually increases due to the higher weights for

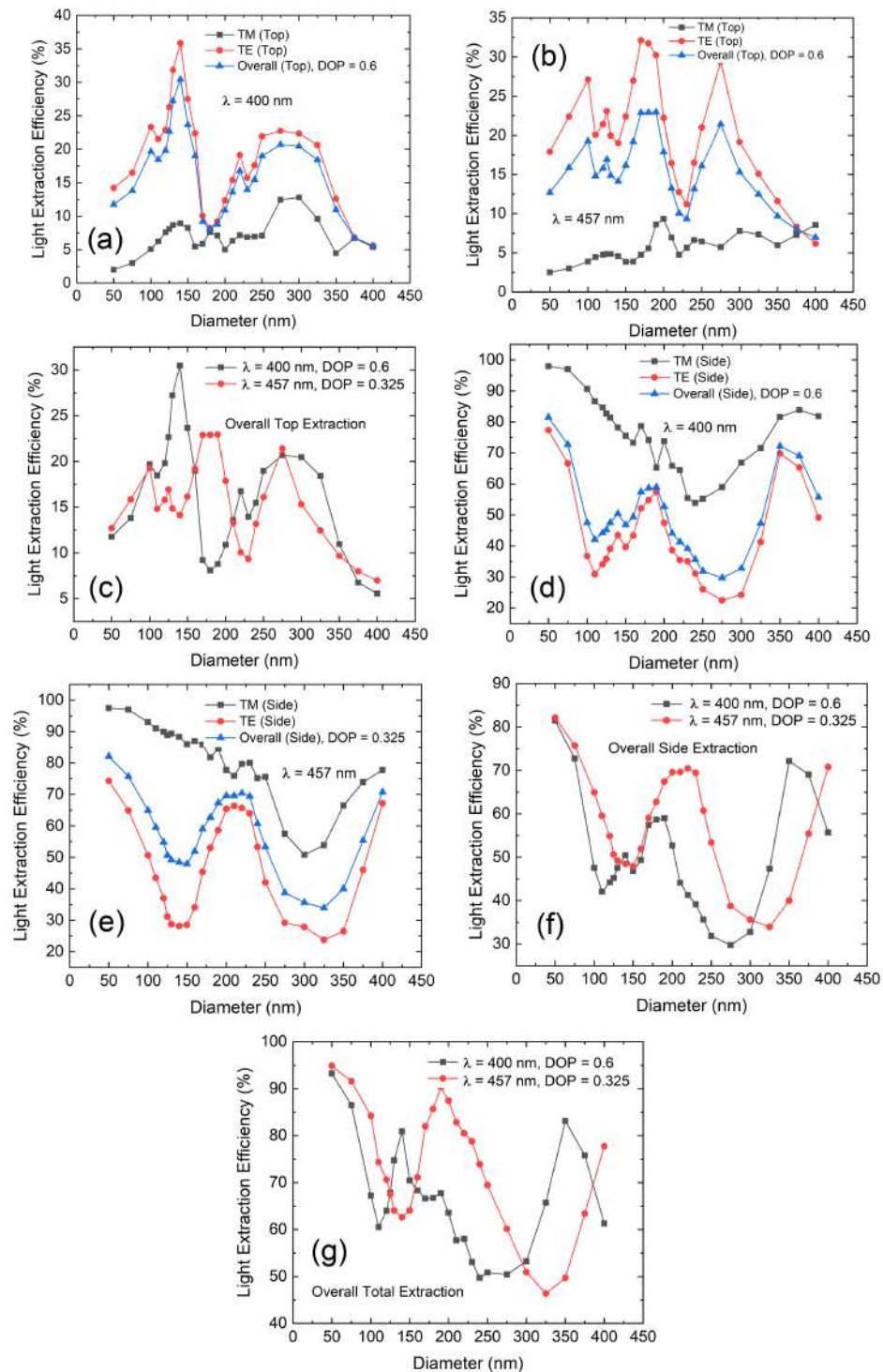


Figure 5.3: Top Extraction at (a) 400 nm and (b) 457 nm for InGaN nanowire LED and (c) comparison between the top efficiencies for these two wavelengths. Side Extraction at (d) 400 nm and (e) 457 nm for InGaN nanowire LED and (f) comparison between the side efficiencies for different wavelengths. (g) Comparison between the total efficiencies for 400 nm and 457 nm wavelengths.

TM polarization and relatively higher side extraction for TM polarization. The effect of DOP variation is much more evident in Figure. 5.4. We have considered five different wavelengths of 400 nm, 410 nm, 415 nm, 447 nm and 457 nm in our studies. The DOP values are shown in table 5.1. With increasing emission wavelengths, the weight of TE polarization reduces, and the weight of TM polarization increases. As shown in Figure. 5.4, the peaks shift to higher wavelengths, and we can observe a gradual reduction in the maximum top extraction as we increase the emission wavelength. On the other hand, we notice the gradual increase of side and total extraction along with the peak shift with the increase of emission wavelength.

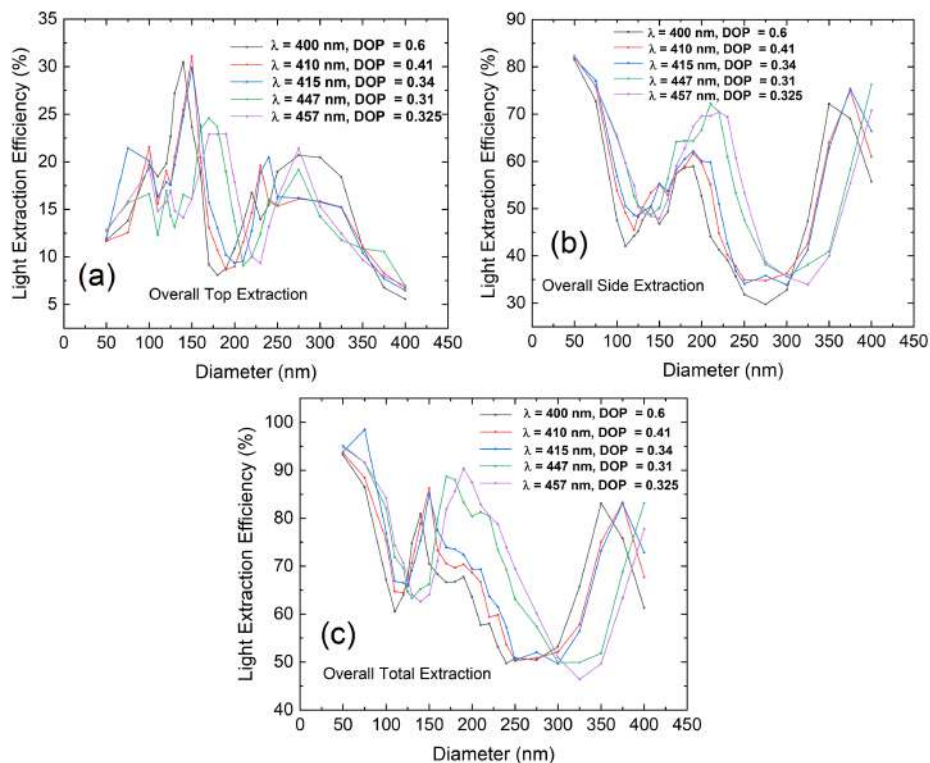


Figure 5.4: Effect of DOP variation with wavelength. (a) top, (b) side and (c) total extraction efficiencies considering DOP values for emission wavelength at 400 nm, 410 nm, 415 nm, 447 nm and 457 nm.

5.2 LEE of AlGaIn-Based DUV LED Considering DOP

In our simulation, we explored AlGaIn/AlGaIn MQW LED structure operating in the wavelength range of 240-320 nm. The DOP value is taken from various literature and calculated from polarization-resolved electroluminescence spectra. DOP values in the wavelength range of 250-320 nm are listed in table 5.2. At lower wavelengths, the optical polarization is mainly TM polarized; hence, DOP value is negative. However, with

increasing wavelength and Al content in the AlGa_N, the polarization nature changes, and a fraction of TE polarized light increases, as shown in Figure. 5.5 due to the rearrangement of the band structure. For emission wavelength at 320 nm, the reported DOP value is positive, indicating the dominant TE-polarized nature of emission.

Table 5.2: DOP and the ratio of TE and TM polarization intensities for several emission wavelengths for AlGa_N-based LED devices [90].

| Wavelength (nm) | DOP | I_{TE}/I_{TM} |
|-----------------|-------|-----------------|
| 250 | -0.4 | 0.428571429 |
| | -0.3 | 0.538461538 |
| | -0.15 | 0.739130435 |
| 290 | -0.1 | 0.818181818 |
| 310 | -0.2 | 0.666666667 |
| 315/320 | 0.3 | 1.857142857 |

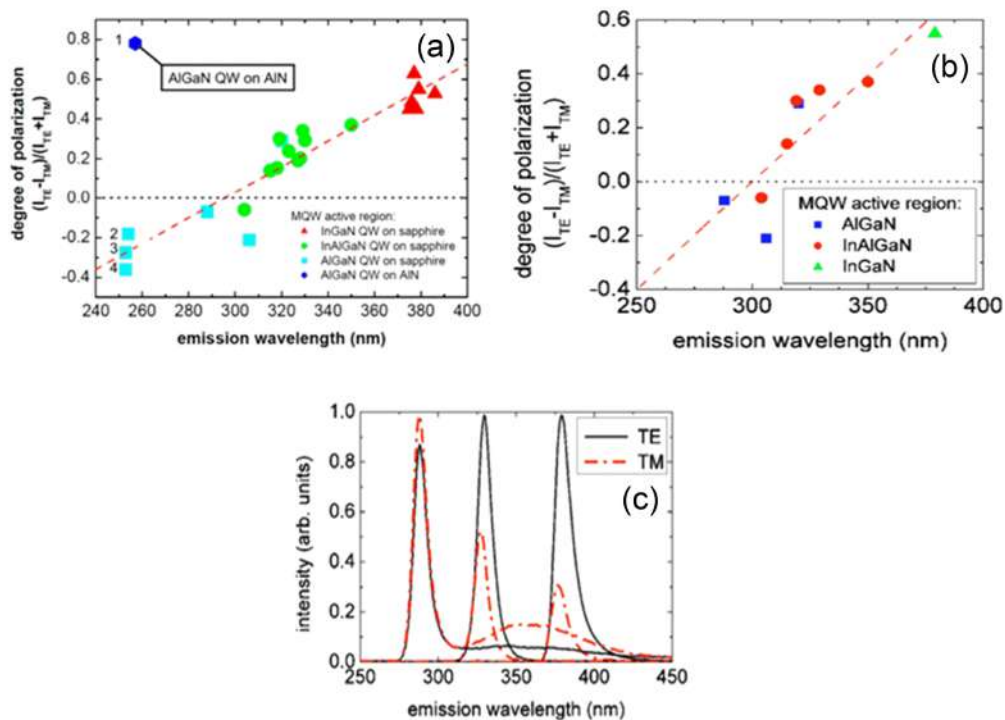


Figure 5.5: (a), (b) Degree of polarization calculated from in-plane electroluminescence as a function of wavelength for several group III-Nitride LEDs. (c) Optical intensity of in-plane emission for different group III-nitride LEDs [44, 89].

Firstly, for an AlGa_N-based LED with an emission wavelength at 250 nm the reported DOP values are -0.4, -0.3 and -0.15 (Figure 5.5(a)). These DOP values refer to TE and TM polarized intensities ratios equal to 0.43, 0.54, and 0.74. From the DOP value, we notice that the polarization nature at 250 nm wavelength is mainly TM polarized due to the negative DOP value. According to the definition of DOP, a more negative DOP

value represents a stronger TM-polarized nature. Firstly, we will consider DOP value equal to -0.4 to elucidate the effect of DOP on LEE. As evident from the negative DOP value, top, side, and total extraction will be dictated more by the top, side and total extraction obtained for TM polarization. This is clearly illustrated in Figure 5.6(a)-(c). As the extraction efficiency is a weighted sum of the efficiencies calculated for TE and TM polarizations, the efficiency is less than the calculated for TM polarizations and more than the calculated value for TE polarizations (Figure 5.6(a)-(c)). So, calculating efficiencies without considering DOP and only considering TM polarizations would overestimate the efficiency values. We observe that efficiencies calculated using DOP

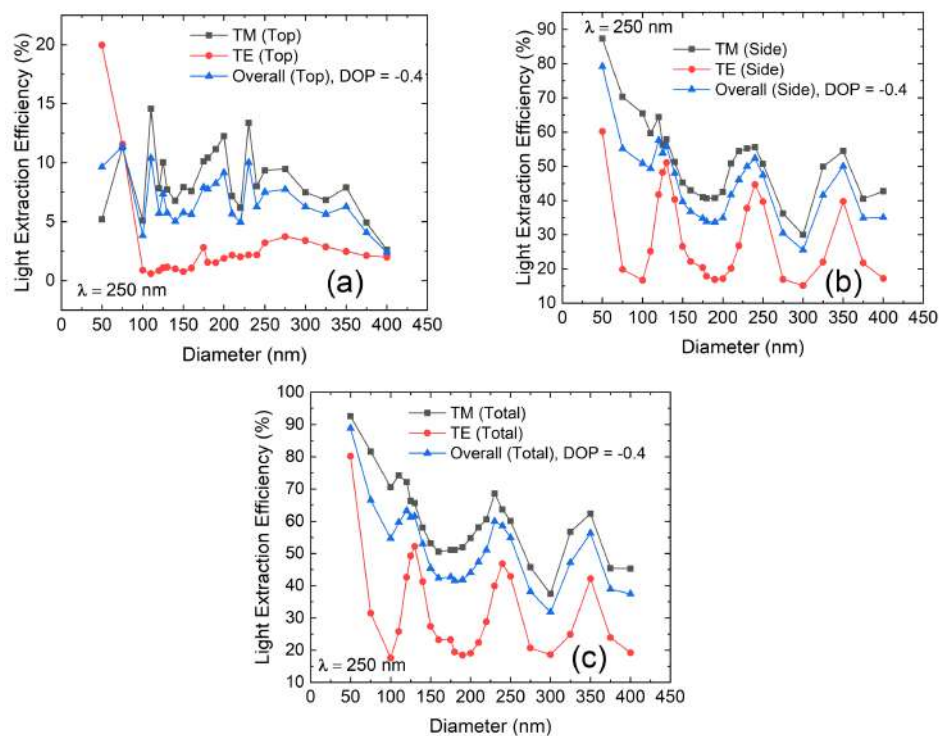


Figure 5.6: Calculation of LEE of AlGaIn nanowire LED using DOP values. (a) Top, (b) side, and (c) total extraction for DOP = -0.4 at a wavelength of 250 nm.

match more closely to the values reported for TM polarizations. Also, the efficiency curves closely mirror those of TM polarizations with the same trends and peaks at the same wavelength range. The maximum values for top, side and total extraction are 11.4%, 75.8% and 87.3%, which are less than those reported considering only TM polarizations. As we mentioned earlier that the actual polarization nature is not purely TE or TM; this method of calculating efficiencies using DOP value is more accurate and consistent with the experimental results.

5.2.1 Effect of DOP Variation

The reported DOP values for AlGaN LED operating at 250 nm are -0.4, -0.3 and -0.15, respectively. Here we will study the effects of DOP variation for calculating LEE of AlGaN nanowire LEDs. As the DOP value becomes less negative, the ratio of TE and TM polarization intensities increases. With increasing DOP, the relative strength of TE polarization increases, which affects the overall extraction efficiencies as shown in Figure 5.7.

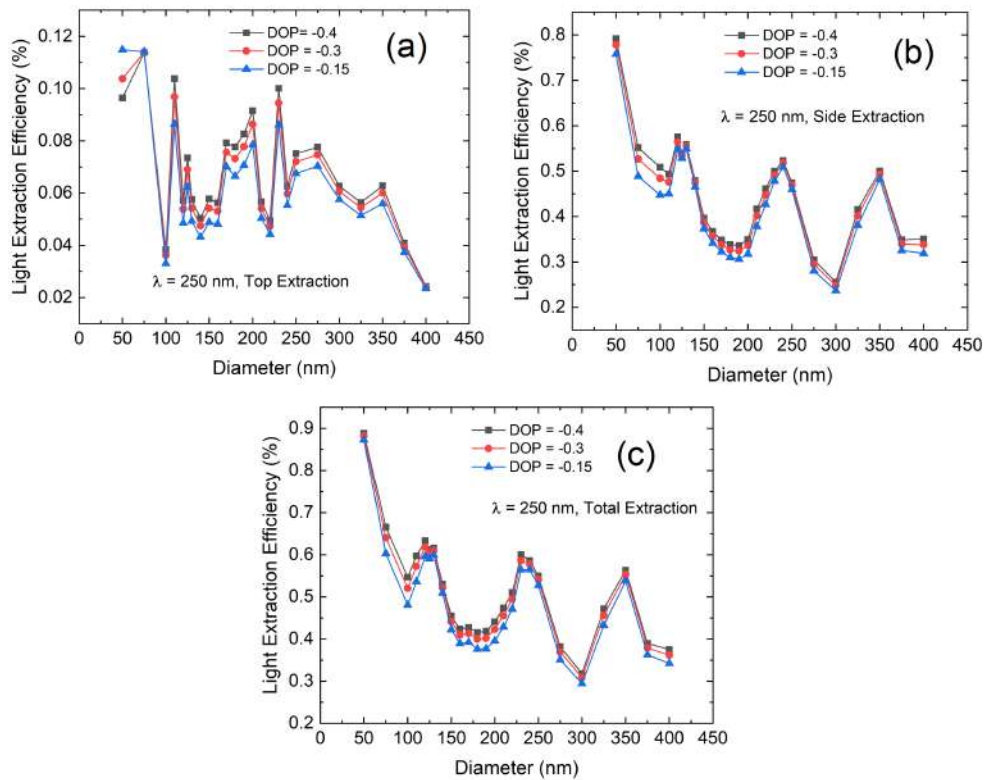


Figure 5.7: (a) Top, (b) side and (c) total extraction efficiency considering DOP values of -0.4, -0.3 and -0.15, respectively.

5.2.2 Effect of DOP Variation with Wavelength

One key point is that DOP for AlGaN LED is not constant but rather varies with emission wavelength. As the Aluminium content in the AlGaN active layer changes, the band structure of the material and hence the emission polarization also varies. It has been reported that there is a transition from dominant TM polarization to dominant TE polarization for higher wavelengths. For AlGaN MQW based LED structure, it has been reported that DOP value changes from -0.4 (250 nm) to 0.3 (320 nm). This illustrates the change of the optical polarization with emission wavelength. Due to the

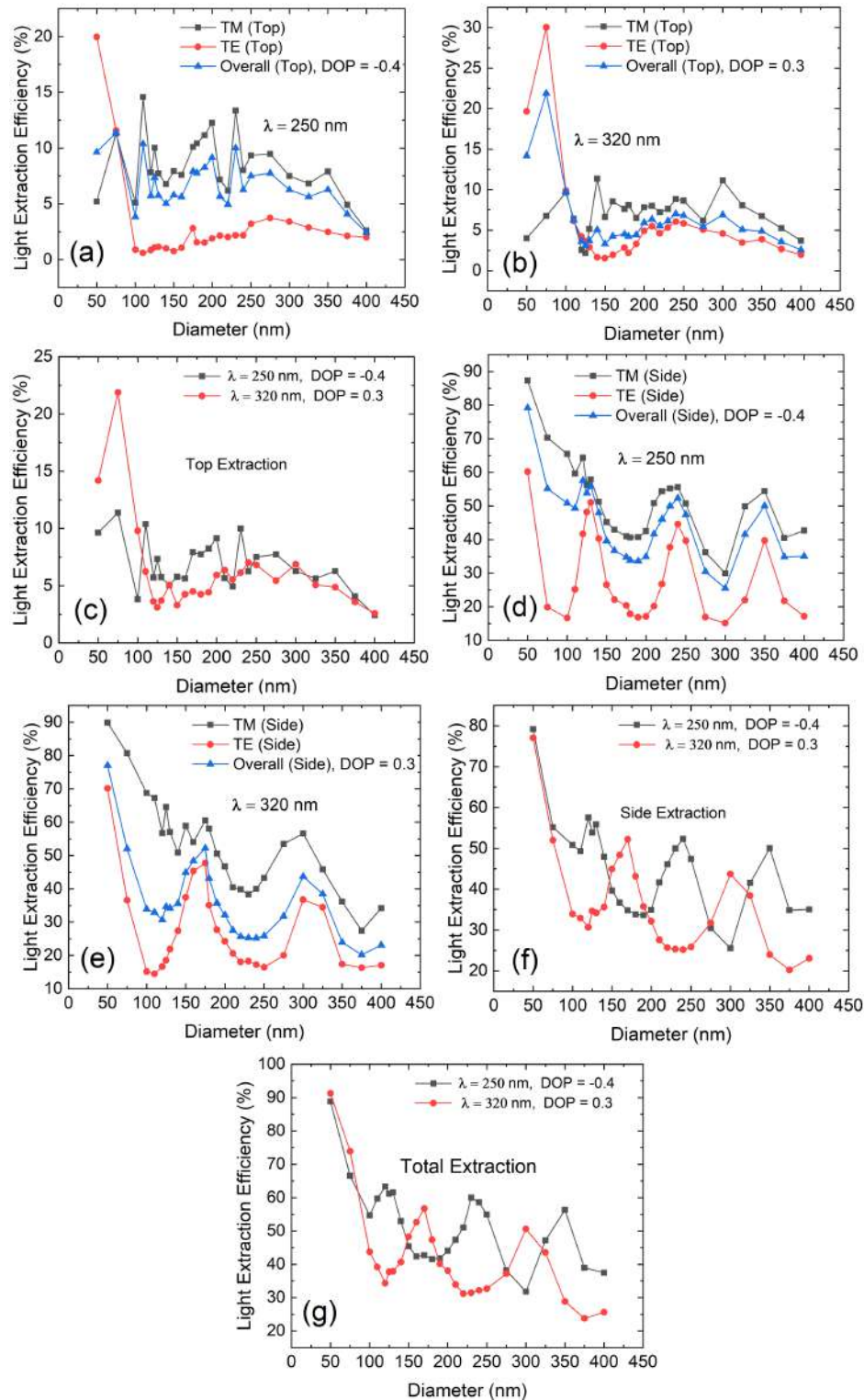


Figure 5.8: Top Extraction at (a) 250 nm and (b) 320 nm for AlGaIn nanowire LED and (c) comparison between the top efficiencies for different wavelengths. Side Extraction at (d) 250 nm and (e) 320 nm for AlGaIn nanowire LED and (f) comparison between the side efficiencies for different wavelengths. (g) Comparison between total extraction efficiencies for 250 nm and 320 nm wavelengths.

change in the optical polarization characteristics, the side, top and total extraction is also modified, which will be studied extensively in this study.

Top extraction efficiencies for 250 nm and 320 nm emission wavelength are shown in Figure 5.8. For DOP = -0.4 at 250 nm, the top extraction more closely follows the top extraction for TM polarization. Similarly, for DOP = 0.3 at 320 nm, the dominant polarization nature is TE and hence the extraction curve follows the curve for TE polarization. We also know that the top extraction for TE polarization in most of the nanowire diameter range is less than TM polarization. Hence, as shown in Figure 5.8, the top extraction at 320 nm is relatively less than that at 250 nm for most of the diameter range. Although the maximum extraction is obtained at 250 nm for nanowire diameter = 75 nm due to high top extraction for TE polarization.

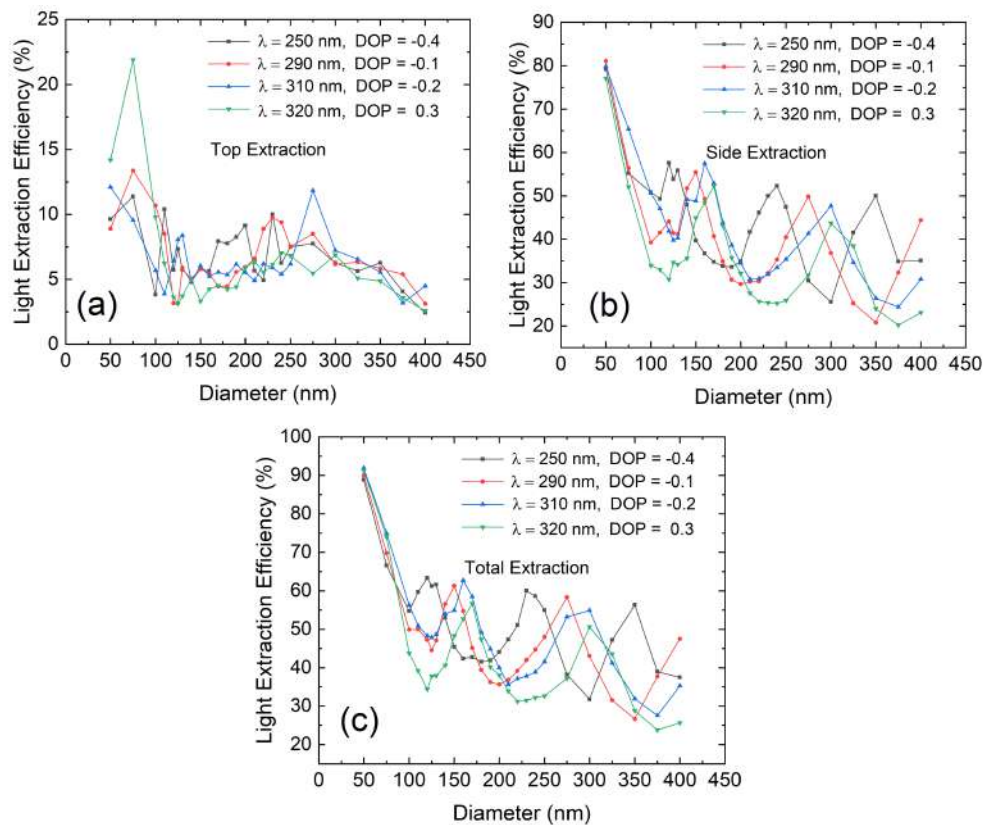


Figure 5.9: Effect of DOP variation with wavelength. (a) top, (b) side and (c) total extraction efficiencies considering DOP values for emission wavelength at 250 nm, 290 nm, 310 nm and 320 nm.

Similarly, side and top extraction curves also follow those curves for TM polarization at 250 nm and TE polarization at 320 nm more closely. Some interesting observations are made in these figures. For the side extraction, although the extraction values remain in the same range, we observe that the peak values shift to higher wavelengths with increasing emission wavelengths. This is also quite intuitive because the side extraction

characteristic is determined by the waveguiding modes. And the mode cut-off radius for several waveguiding modes shifts to higher wavelengths with increasing emission wavelength. This results in the right shift of the peaks in the side extraction curve. Total extraction is just the summation of side and top extraction. And, due to loss in the top p-GaN contact layer, the top extraction is quite low and hence the total extraction is dominated by the side extraction. So, the value of the total extraction, just like the side extraction case, remains within the same range, but peaks shift to a higher wavelength for 320 nm. Reported DOP values for different emission wavelengths are shown in Table 5.2, which once again highlight the transition of the optical polarization from TM polarized nature to TE polarized nature. We observe in Figure 5.9(a) that top extraction values remain in the same range between 4-10% for most of the diameters and still exhibit relatively lower values. Maximum top extraction of 21% is observed for emission wavelength at 320 nm for a nanowire diameter of 75 nm. Also, the top extraction value reduces with increasing emission wavelength for most diameters. Side and total extraction curves exhibit oscillatory behaviour and the values for side extraction range from 25% to 60% for larger diameters. Similarly, the range of total extraction is between 30% to 65%. The gradual shift of the peaks is better illustrated in Figure 5.9 (b)-(c), where observe the right shift of the peaks with emission wavelength.

Chapter 6

Effect of Array Periodicity

So far in our simulation study, we only considered isolated nanowires as the overall extraction will be governed by each individual nanowire. However, in practical settings, there will be an array of nanowires combined to form a micro-LED device. A significant advantage of nanowire LEDs as compared to bulk-micro LEDs is the less material absorption and higher relative extraction efficiencies. Several different phenomena and conditions then become crucial while considering an array of nanowires rather than a single nanowire. In this section, we will investigate extensively the effect of array periodicity i.e. the distance between the nanowires, g , which is defined in Equation 3.12. Furthermore, we will propose the optimized design in terms of array periodicity for maximizing the top, side and total extractions for InGaN-based and AlGaIn-based nanowire LEDs.

6.1 InGaN LEDs

We first studied the effect of array periodicity/ distance between the nanowires in a square periodic nanowire assembly on the LEE for InGaN-based nanowire array-based micro LEDs. We limited our study to designing optimized structural parameters i.e. nanowire diameter and array periodicity for maximizing top extraction to a single wavelength of 400 nm. In our simulation, a unit cell is simulated with periodic boundary condition and the distance between the nanowires represent the actual gap between the nanowires. Furthermore, we only studied the light extracted on the top side of the nanowire assembly.

The top extraction for TM polarization as shown in Figure 6.1, is almost negligible for smaller nanowire diameters and distances. We analyzed the radiation pattern for

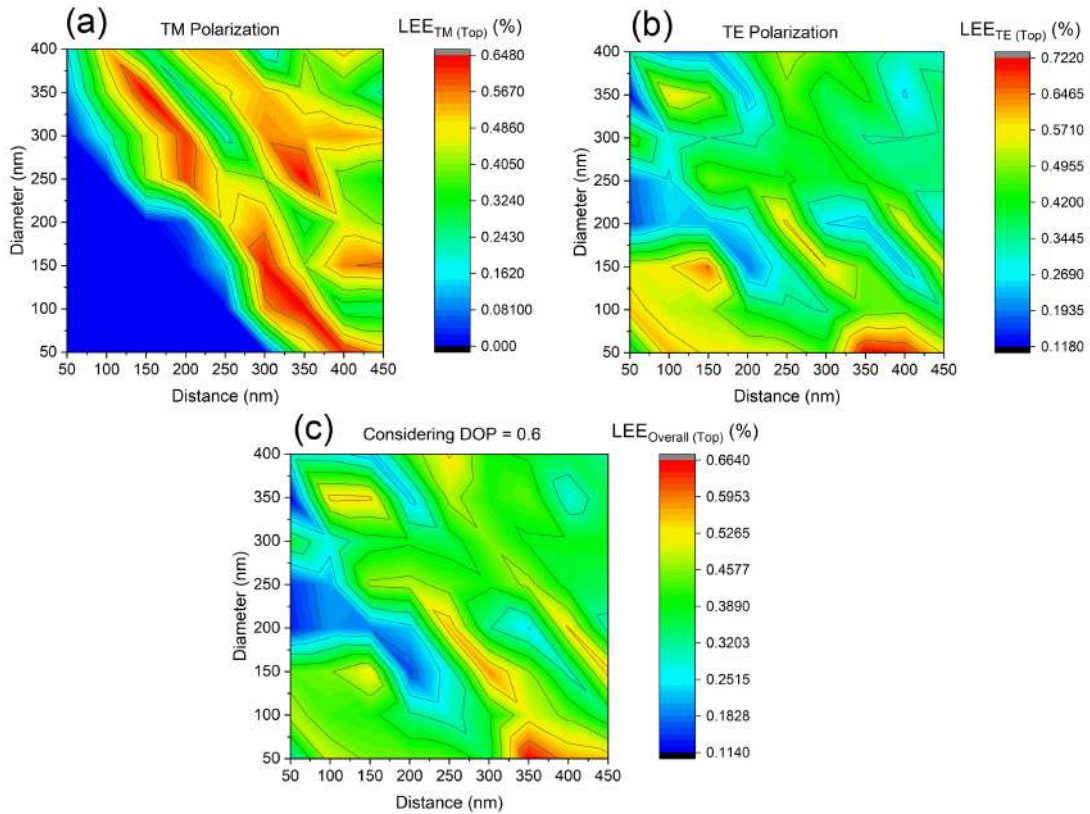


Figure 6.1: LEE on top for different InGaN nanowire diameters and distances for (a) TM polarization, (b) TE polarization, and (c) considering DOP.

different nanowire diameters and distances to explain their influence on extraction. The radiation pattern depends on the nanowire diameter as well as the distance between the nanowires. Light emitted from the nanowire emitters bounces back after being reflected from the neighbouring nanowires and forms localized modes in between the nanowires. Moreover, the band gap of the periodic structure also plays a crucial role in the overall extraction. If both the nanowire diameter and distance are small, then light gets confined within the nanowire and the surrounding region. So, light can't be extracted from the top side which severely limits the top extraction efficiency. This is clearly illustrated in the Figure 6.2(a) for nanowire diameter = 50 nm and distance = 100 nm. However, with nanowire diameter = 50 nm and distance = 400 nm, top extraction as high as 57% can be achieved. The radiation pattern (Figure 6.2(b)) illustrates that the E-field is no longer confined within the nanowire and surrounding region rather, this light can be extracted from the top side. As we increase the spacing between the nanowires, the nanowire acts more like an isolated nanowire and the effect of the neighbouring nanowire diminishes. Although with larger spacing in between the nanowires, the efficiency is improved but it requires a larger area for the same amount of light output. Just like smaller nanowires, nanowires with larger diameters are also affected by the spacing between the nanowires.

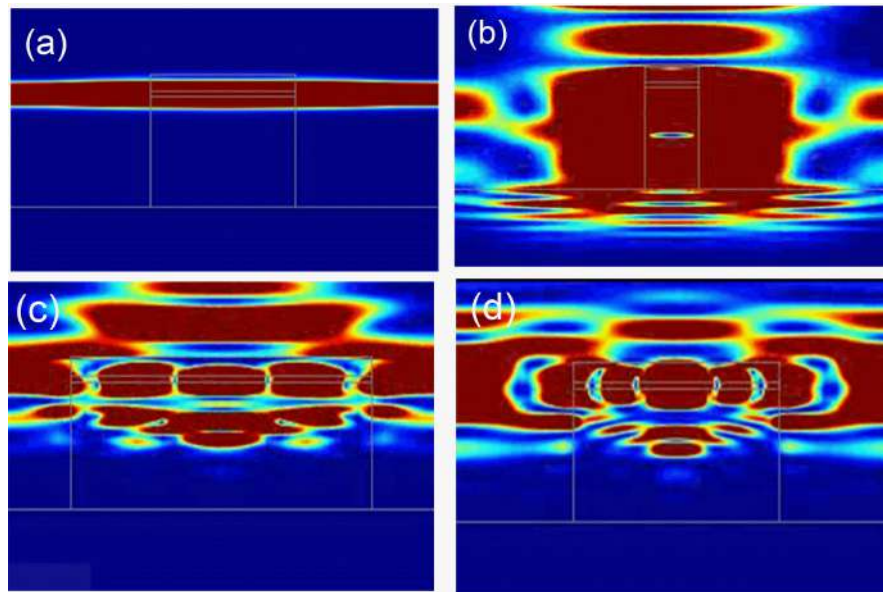


Figure 6.2: Electric field pattern (TM polarization) for diameter = 50 nm and (a) distance = 100 nm, (b) distance = 400 nm. Radiation pattern for diameter = 350 nm and (c) distance = 150 nm and (d) distance = 400 nm.

As can be evident from Figure 6.1, the top extraction can vary by huge amounts for small changes in the spacing. The radiation pattern for nanowire diameter = 350 nm having two different spacing of 150 nm and 400 nm are illustrated in Figure 6.2(c)-(d). The top extraction reduces from 53% to 28% as increase the spacing from 150 nm to 400 nm. We can see that for spacing of 150 nm, top extraction is relatively higher because most of the light can be extracted from the top and is not confined. However, for spacing = 400 nm, a significant portion of emission is trapped within the spacing and can't be extracted from the top. The maximum top extraction that can be achieved for TM polarization is 64% for diameter = 100 nm and spacing = 350 nm. Most importantly, in the case of isolated nanowires light emitting from the active region will be absorbed by the surrounding absorption layer which limits top extraction; however, in the case of an array of nanowires light can be reflected from the neighbouring nanowire surfaces and can be collected from the top side. For TE polarization relatively higher top extraction is possible even for smaller nanowire diameter and spacing (Figure 6.1(b)). Top extraction in the range of 30-55% can be achieved for most of the nanowire diameters and spacing. High and low extraction can be explained by the radiation pattern. The maximum top extraction for TE polarization is 72% which is higher than that for TM polarization.

The maximum top extraction is achieved for diameter = 50 nm and spacing = 400 nm. The radiation pattern for some different configurations are shown in Figure 6.3(a)-(d). Even for smaller nanowire diameter and spacing, top extraction can be quite high for TE polarization as shown in Figure 6.3 (a). For a nanowire diameter of 150 nm, changing

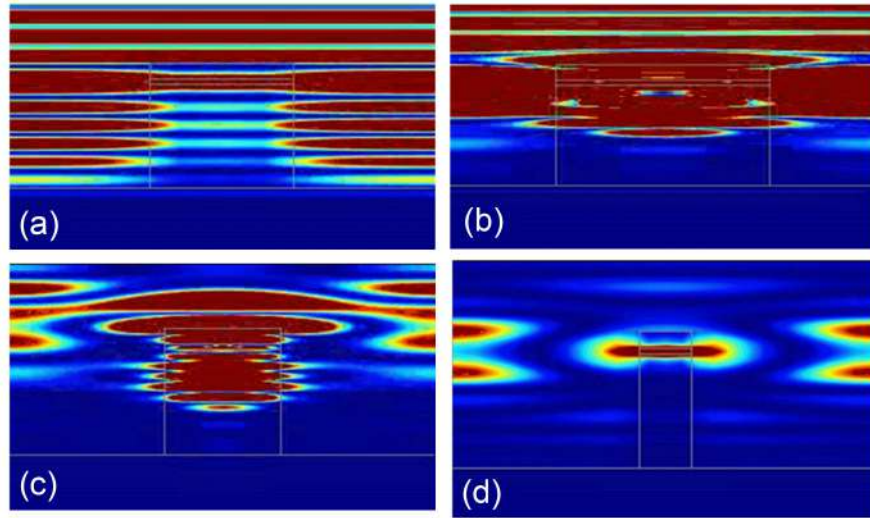


Figure 6.3: Electric field pattern (TE polarization) for (a) diameter = 50 nm, distance = 100 nm, and (b) diameter = 150 nm distance = 150 nm. Radiation pattern for (c) diameter = 150 nm, distance = 400 nm and (d) diameter = 50 nm, distance = 400 nm.

the spacing from 150 nm to 400 nm can severely influence the top extraction as evident in Figure 6.2 and Figure 6.3. The top extraction experience a 45% reduction due to the change in spacing, and the E-field pattern for these two different spacing are shown in Figure 6.3(b)-(c). For nanowire diameter = 50 nm and spacing = 350 nm, we observed the maximum top extraction of 72%. For wavelength 400 nm, DOP is 0.6 which describes the TE dominant nature of polarization. Hence, the extraction calculated considering DOP will mostly follow that of TE polarization as shown in Figure 6.1(c). The maximum top extraction considering DOP = 67% which is higher than that for TM polarization but lower than that for TE polarization. From our simulation, we propose that a nanowire array of diameter = 50 nm and spacing = 350 nm will exhibit the maximum top extraction.

6.2 AlGaIn-Based Nanowire LEDs

In this section, we will study the influence of diameters and spacing on the top extraction of AlGaIn-based nanowire LEDs. The underlying principle behind extraction values is the same as that for the InGaIn-based nanowire LEDs. So, we will only analyze the extraction characteristics with structural parameters without analyzing the radiation patterns in detail. We have set the emission wavelength at 250 nm in the UV-C region, and similar studies can be done for other wavelengths also. For smaller nanowire diameters and distances, the top extraction is almost negligible for TM polarization. However, increasing the spacing between smaller nanowires improves the top extrac-

tion by reducing the impact of neighbouring nanowires. For nanowire diameter = 50 nm and spacing of 350 nm, we observe the maximum extraction of 46%. Top extraction varies in the range of 10-30% for most of the combinations of diameters and spacing. For the TE polarization, we notice that top extraction is quite small for larger diameters. It's due to the presence of the top p-GaN contact layer and for larger diameters, a significant amount of light is absorbed in the top layer which reduces the top extraction greatly. However, a very high top extraction of about 70% can be achieved at smaller diameters. We observe maximum top extraction of 70% for a nanowire diameter of 50 nm and spacing = 450 nm. Due to the TM dominant polarization nature, the top extraction curve closely follows that of TM polarization. Considering DOP, the maximum extraction is 48% for diameter = 50 nm and spacing = 450 nm. So, in order to maximize top extraction for AlGaIn-based nanowire LEDs, a diameter of 50 nm and spacing equal to 450 nm should be considered.

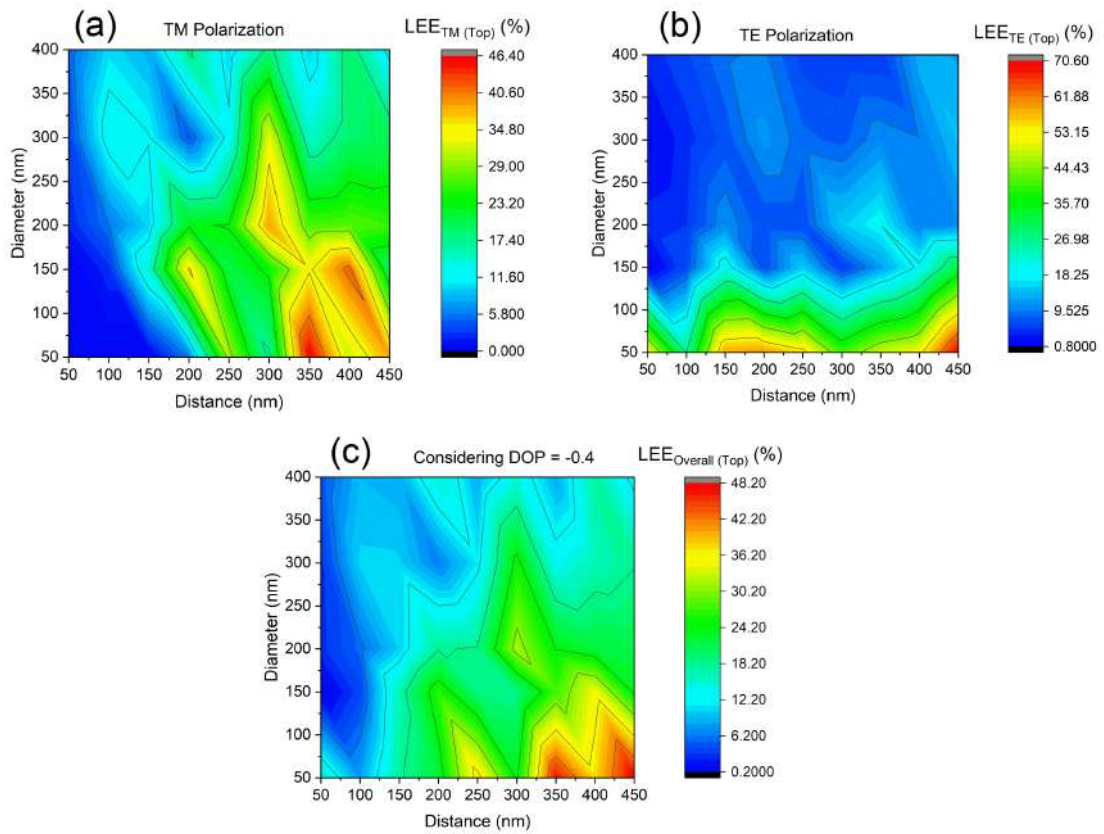


Figure 6.4: LEE on top for AlGaIn-based LEDs for different nanowire diameters and distances for (a) TM polarization, (b) TE polarization, and (c) considering DOP.

Chapter 7

LEE Improvement

Several methods have been proposed to enhance the LEE of nanowire-based and planar micro-LEDs, such as the addition of metal plates, inclined side reflectors, textured surfaces, anti-reflective coating, and plasmonic and photonic structures. In this section, we will mainly discuss the impact of metal plates and inclined reflectors on the LEE of these emitters.

7.1 Influence of Bottom Metal Plate for Single InGaN nanowire

In our study, a single InGaN nanowire is considered, and an Al metal plate is placed at the bottom of the nanowire as shown in Figure 7.1. We considered the nanowire diameter to be 140 nm due to high top extraction for this particular diameter at wavelength 400 nm. The thickness of the bottom metal layer is also varied to understand the relationship between the metal thickness and LEE enhancement. From our previous analysis, we found that a significant amount of emitted light passes through the substrate and gets absorbed. The placement of a metal reflector reflects some light in the upward direction and hence improves the extraction efficiency. From Figure 7.2, we can see that LEE is significantly improved due to the inclusion of a bottom metal reflector. We also examined the effect of the metal thickness on overall LEE and the LEE enhancement for different metal thicknesses is shown in Fig. 7.2. The effect of metal thickness variation on the upward reflection or overall LEE enhancement is minimal and we observe an average LEE enhancement of 28% after the introduction of approximately 50 nm thick metal reflector. As shown in Figure 7.2, there is a slight variation in the LEE enhancement with a metal thickness which results from the slight variation

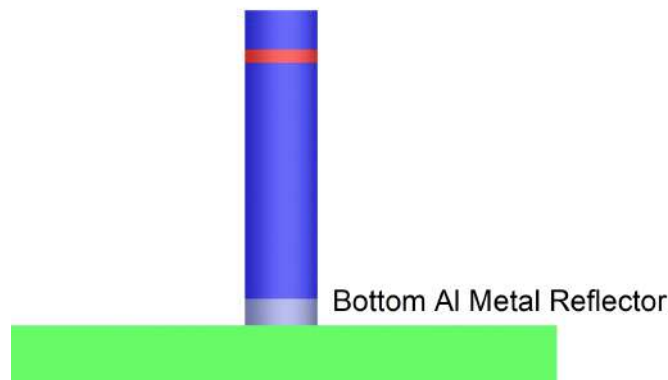


Figure 7.1: A schematic of single InGaN nanowire LED with bottom Al metal plate for LEE enhancement.

in the light emitted along the sideways direction.

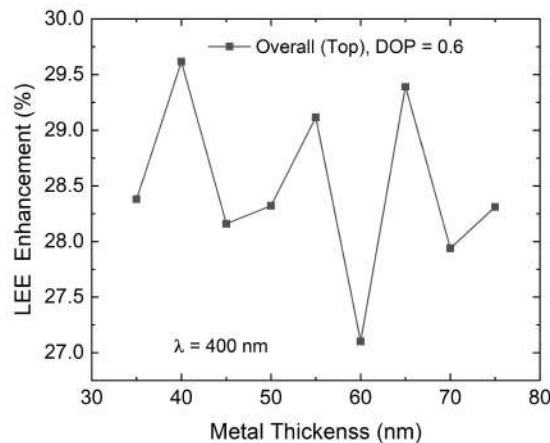


Figure 7.2: Percentage LEE enhancement due to the introduction of bottom reflector.

7.2 Effect on AlGaIn-based single nanowire LED

Similarly, we placed an Al bottom metal layer inside the AlGaIn-based single nanowire emitter to understand the effect of metal layer thickness on LEE enhancement. AlGaIn nanowire diameter was set to 250 nm, and the emission wavelength was set at 250 nm.

The influence of metal layer thickness on AlGaIn single nanowire emitters is also examined in detail. For TM polarization, top extraction exhibits oscillatory behaviour with the maximum enhancement of 13.5% achieved for metal thicknesses of 50 nm and 150 nm. The dip in the top extraction corresponds to the increase in the side extraction. The top extraction for TE polarization reduces with the introduction of the metal layer due to absorption in the top p-GaN layer. Side extraction enhancement as high as 35% can

be observed for the TE polarization case. We see an overall top extraction enhancement of 2.5% while considering the DOP reported for this particular wavelength. We can achieve maximum top extraction of almost 10% with 50 nm metal thickness.

7.3 Effect of Inclined Side Reflector on InGaN Nanowire Array LED

Besides metal reflectors, another method for LEE enhancement is the addition of inclined side reflectors. The side reflectors deflect the light emitting sideways towards the top direction and hence improve the top LEE. In order to understand the effect of these side reflectors, a periodic nanowire assembly is considered with nanowire diameter = 150 nm and periodicity = 300 nm. A side wall reflector with an Al metal reflector

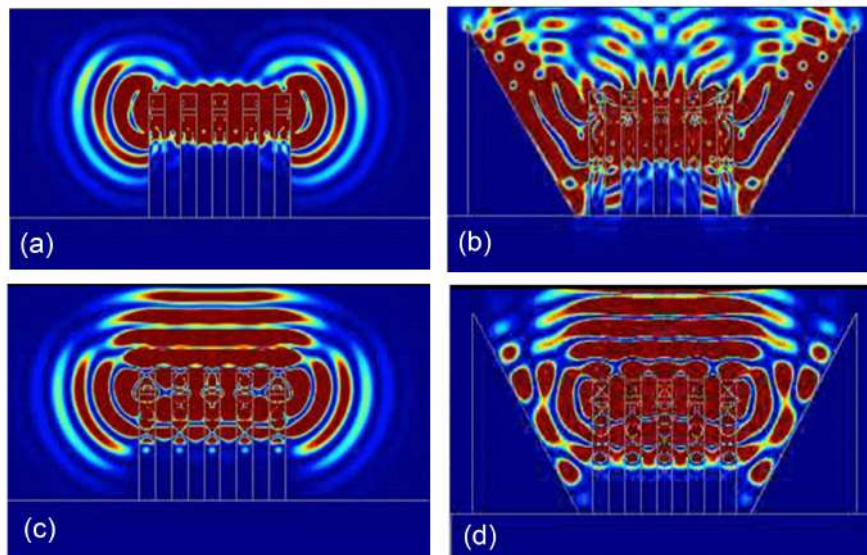


Figure 7.3: Radiation pattern for InGaN-nanowire array-based micro LEDs for TM polarization (a) without and (b) with inclined sidewall reflectors. Emission pattern for TE polarization (c) without and (d) with inclined side reflectors.

with a triangular cross-section, is inserted surrounding the nanowire array structure for guiding the light in the upwards direction. Figure 7.3(a)-(b) shows the radiation pattern with and without the reflectors for TM polarization and the effect of side reflectors will be significant for TM polarization because most of the light emits sideways without the reflectors. The top LEE enhancement due to side reflectors for TM polarization is found to be more than 50% which is very significant. Due to the radiation pattern for TE polarization, the effect of inclined side reflectors is relatively less for the TE polarization (Figure 7.3).

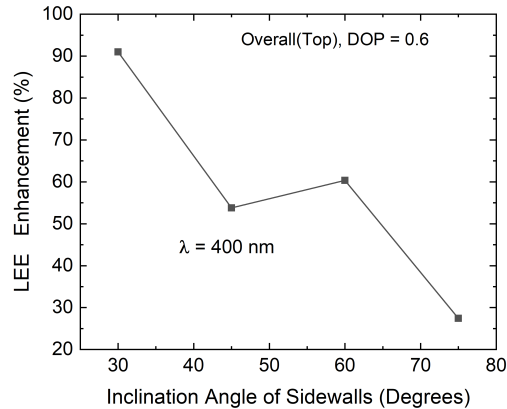


Figure 7.4: Percentage LEE enhancement with inclination angle of the sidewall reflectors.

Moreover, the percentage of emitted light reflected downward and upward depends on the inclination angle of the sidewalls, as shown in Figure 7.4. We varied the inclination angle from 30 to 75 degrees, and we observed a downward trend of LEE enhancement with an increasing inclination angle. With a high inclination angle, the percentage of light reflected downward increases and hence, overall extraction at the top diminishes. We have observed almost 90% LEE enhancement due to the introduction of inclined side reflectors having an inclination angle of 30 degrees. Thus, inclined side reflectors can significantly affect the LEE characteristics of nanowire-based LED devices.

7.4 Effect of Inclined Side Reflector on AlGaIn Nanowire Array and Micro LEDs

Similarly, the impact of the inclined side reflectors on the LEE enhancement for AlGaIn nanowire array-based micro-LEDs is also studied extensively. The overall effect of the side reflectors is greater for AlGaIn-based LEDs due to the strong TM polarization nature. In our study, the nanowire diameter = 50 nm and periodicity = 400 nm are set according to the optimized structural parameters. Top LEE enhancement for TM polarization and TE polarization are found to be 11% and 5%, respectively. Moreover, considering DOP, the enhancement is calculated to be 9%. The E-field distribution pattern for AlGaIn micro-LED devices operating at UV-C for different optical polarizations is shown in Figure 7.5. We obtain an enhancement factor of 30% and 12% for TM and TE polarizations with the introduction of inclined side Al reflectors. So, the introduction of inclined side wall reflectors also significantly improves the top extraction

characteristics.

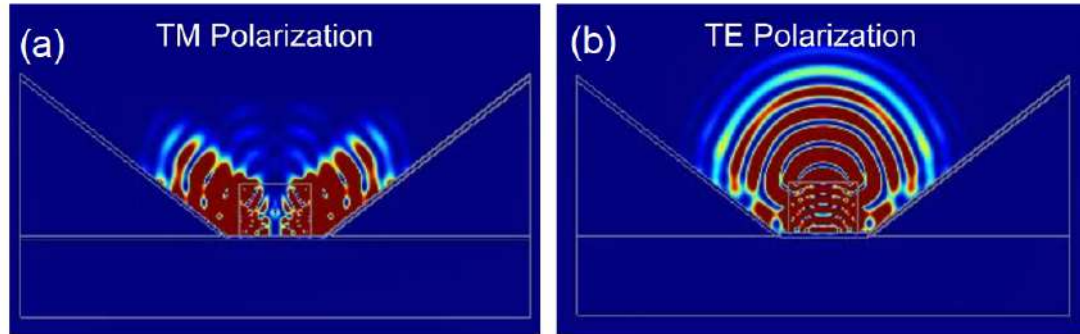


Figure 7.5: Emission pattern for AlGaIn micro UV-C LEDs with inclined Al side reflectors for (a) TM polarization and (b) TE polarization [56]

7.5 Comparison among different enhancement methods

In this section, we will compare the performance of several enhancement methods. The inclined side wall reflectors outperform the bottom metal reflector. LEE enhancement as high as 90% can be achieved with a 30-degree inclination angle, whereas we can only achieve LEE enhancement of 28% with a 50 nm thick bottom metal reflector layer. However, fabricating a nanowire LED device with a bottom metal reflector is much simpler than an inclined side wall reflector with a triangular cross-section. We have already reported several LEE enhancement methods: surface roughening, substrate engineering, and surface-plasmon enhancement in Section 2.9.

Table 7.1: Comparison among different LEE enhancement methods.

| Methods | LEE Enhancement (%) |
|---|---------------------|
| Bottom Metal Reflector | 28 |
| Inclined Side Reflector | 90 |
| Surface Roughening (p-GaN microdome) [74] | 36.8 |
| Optimal PC Structure [79] | 19 |
| Silica/ Polystyrene Lens Array [80] | 219 |
| Textured ITO with Ag nanoparticle [81] | 20.2 |

It has been reported that introducing a p-GaN micro dome structure with nanorod can enhance LEE by 36.8% [74]. Utilizing optimal photonic crystal (PC) structure, the LEE has been reported to be 19% and 14% for blue and UV LEDs [79]. Ee et al. demonstrated 219% enhancement of light output power by using Silica/ polystyrene lens array [80]. Moreover, it has been reported that textured ITO with Ag nanoparticle can enhance light output power by 20.2% [81]. Additionally, nanopatterned substrates

and surface plasmon methods have been utilized to significantly boost LEE enhancement. Fabrication devices with nano-structured roughness, nanopatterned substrates and complex PC structures require complicated nanofabrication processes and tools, whereas the insertion of reflective layers can be an alternative to LEE enhancement in a much simpler way. Moreover, these approaches can be coupled with our LEE enhancement methods. In this thesis, we only simulated basic LED devices and studied the impact of two external enhancement methods considering optical polarizations. In addition to surface roughening, substrate engineering, and surface plasmon methods, the application of reflectors can boost overall LEE even more.

Chapter 8

Conclusions

8.1 Conclusions

The key findings of this thesis are as follows:

Side, top and total LEE of InGaN and AlGaN single nanowire LEDs operating in visible and UV wavelength regions are evaluated using FDTD optical simulations. The simulation setup, methodology and structural modelling of these LED devices are described in detail. The impact of emission polarization on top, side and total extractions is analyzed using waveguiding nature of these nanostructures. The LEE of InGaN and AlGaN nanowire LEDs is more accurately estimated using DOP. A weighted average method was proposed to calculate LEE considering DOP from the LEE values obtained for TE and TM polarizations. This method can be generalized to estimate LEE more accurately for any LED devices with known emission polarization characteristics. Moreover, the dependence on LEE with nanowire structural parameters has been reported. Considering DOP and material absorption, the maximum calculated top, side, and total extraction efficiencies for a single AlGaN nanowire LED operating at 250 nm are 11.4%, 75.8% and 87.3%, respectively. Similarly, for a single InGaN nanowire-based LED operating at 400 nm, the maximum top extraction efficiency of 30% is achieved for nanowire diameter of 125 nm. The impact on DOP variation with emission wavelength on LEE is analyzed in detail. A shift in the peak position and a change in the maximum extraction was noticed due to the variation of DOP.

Optimized geometry in order to maximize top extraction for AlGaN and InGaN nanowire array-based micro LEDs is proposed. The impact of nanowire diameter and array periodicity is studied in detail. Considering DOP, we achieved the maximum top extraction of 67% for InGaN nanowire array-based micro LEDs for nanowire diameter and array

periodicity of 50 nm and 350 nm, respectively. Similarly, for our AlGaIn nanowire-array based micro LEDs, our optimized geometry with nanowire diameter and spacing of 50 nm and 450 nm, respectively, exhibits maximum top extraction efficiency of 48%.

Two methods have been used for enhancing the LEE of nanowire and micro LED. The influence of a bottom Al metal reflector for single nanowire AlGaIn and InGaIn LEDs is discussed in detail, and enhancement factors are reported. Moreover, the effect of inclined Al side-reflectors in periodic nanowire arrays and micro LEDs on LEE is also reported. Using our optimized geometry and taking DOP into consideration, the enhancement of top LEE for InGaIn and AlGaIn nanowire array-based LED devices with inclined side reflectors was also calculated.

8.2 Future Potentials of this Research Work

In this work, we estimated the LEE of nanowire and micro LEDs considering DOP and proposed a weighted average method for accurately estimating LEE considering DOP. This method of more accurate LEE calculating using optical simulations and considering emission polarization nature can be generalized for other emitters operating at different wavelength ranges. We only considered a small portion of the UV and visible range in our study. Similar studies can be done for a broader wavelength range spanning from UV to IR using different semiconductor materials and compositions. A more detailed study will be a useful design guide for the design of next-generation highly efficient LED devices. We only explored DOP variation within a small wavelength range; however, a complete study considering DOP in a much larger wavelength range and comparing the reported DOP values is needed. Moreover, the variation of DOP with structural parameters and their overall impact could be an interesting research topic. We proposed an optimized geometry for nanowire array-based LEDs operating at two specific wavelengths and DOPs. However, there is potential to estimate LEE for a broader wavelength range using the methodology of this research. Moreover, the nanowire structure used in this work is rudimentary as we mainly focused more on the estimation and analysis of LEE than maximizing LEE. There have been numerous research works for optimizing nanowire structures and introducing different electrodes, photonic crystals and plasmonic structures to enhance radiation patterns and LEE. Our method can be used to estimate the LEE of these optimized structures and the impact of these modifications on LEE, considering DOP can add to the semiconductor LED design process. We also only considered uniform structure and periodic arrangement. The impact of irregularity in structure and random distribution of nanowire arrays has

not been mentioned in this work. Moreover, only extraction characteristic is considered as a performance metric in this study. However, the directional characteristic of the LED devices is not considered, which is also a very important performance metric. An optimized design for better directional performance can be extremely useful. The position of the device in the nanowire and the height of the nanowire are kept constant. The effect of nanowire height, the shape of the nanowire and the position of the active region on the overall extraction characteristics haven't been explored in detail. Additionally, the LEE performance of SQW nanowires LED devices hasn't been considered and the impact of temperature change on the overall LEE performance hasn't been studied. Also, the impact of DBR mirrors on LEE enhancement can be a promising research topic. A comprehensive study with DFT simulation relating the band structure and LEE can be extremely useful for highly efficient LED devices.

References

- [1] Wu, Y., Liu, X., Pandey, A., Zhou, P., Dong, W.J., Wang, P., Min, J., Deotare, P., Kira, M., Kioupakis, E. et al. "Iii-nitride nanostructures: Emerging applications for micro-leds, ultraviolet photonics, quantum optoelectronics, and artificial photosynthesis." *Progress in Quantum Electronics*, p. 100401, 2022
- [2] Pandey, A. and Mi, Z. "Iii-nitride nanostructures for high efficiency micro-leds and ultraviolet optoelectronics." *IEEE Journal of Quantum Electronics*, volume 58, no. 4:pp. 1–13, 2022
- [3] Zhu, D., Wallis, D. and Humphreys, C. "Prospects of iii-nitride optoelectronics grown on si." *Reports on Progress in Physics*, volume 76, no. 10:p. 106501, 2013
- [4] Chen, C.Y., Zhu, G., Hu, Y., Yu, J.W., Song, J., Cheng, K.Y., Peng, L.H., Chou, L.J. and Wang, Z.L. "Gallium nitride nanowire based nanogenerators and light-emitting diodes." *ACS nano*, volume 6, no. 6:pp. 5687–5692, 2012
- [5] Zhao, C., Alfaraj, N., Subedi, R.C., Liang, J.W., Alatawi, A.A., Alhamoud, A.A., Ebaid, M., Alias, M.S., Ng, T.K. and Ooi, B.S. "Iii-nitride nanowires on unconventional substrates: From materials to optoelectronic device applications." *Progress in Quantum Electronics*, volume 61:pp. 1–31, 2018
- [6] Lee, H.Y. and Kim, S. "Nanowires for 2d material-based photonic and optoelectronic devices." *Nanophotonics*, 2022
- [7] Wasisto, H.S., Prades, J.D., Gülink, J. and Waag, A. "Beyond solid-state lighting: Miniaturization, hybrid integration, and applications of gan nano- and micro-leds." *Applied Physics Reviews*, volume 6, no. 4:p. 041315, 2019
- [8] Nakamura, S. "Current status of gan-based solid-state lighting." *MRS bulletin*, volume 34, no. 2:pp. 101–107, 2009

- [9] Wang, Z., Shan, X., Cui, X. and Tian, P. “Characteristics and techniques of gan-based micro-leds for application in next-generation display.” *Journal of semiconductors*, volume 41, no. 4:p. 041606, 2020
- [10] Koike, M., Shibata, N., Kato, H. and Takahashi, Y. “Development of high efficiency gan-based multiquantum-well light-emitting diodes and their applications.” *IEEE Journal of selected topics in quantum electronics*, volume 8, no. 2:pp. 271–277, 2002
- [11] Yue, Q., Li, K., Kong, F., Zhao, J. and Li, W. “Analysis on the light extraction efficiency of gan-based nanowires light-emitting diodes.” *IEEE Journal of Quantum Electronics*, volume 49, no. 8:pp. 697–704, 2013
- [12] Wang, Z., Zhu, S., Shan, X., Yuan, Z., Qian, Z., Lu, X., Fu, Y., Tu, K., Guan, H., Cui, X. et al. “Red, green and blue ingan micro-leds for display application: Temperature and current density effects.” *Optics Express*, volume 30, no. 20:pp. 36403–36413, 2022
- [13] Zhuang, Z., Iida, D. and Ohkawa, K. “Ingan-based red light-emitting diodes: from traditional to micro-leds.” *Japanese Journal of Applied Physics*, volume 61, no. SA:p. SA0809, 2021
- [14] Khan, A., Balakrishnan, K. and Katona, T. “Ultraviolet light-emitting diodes based on group three nitrides.” *Nature photonics*, volume 2, no. 2:pp. 77–84, 2008
- [15] Shur, M.S. and Gaska, R. “Deep-ultraviolet light-emitting diodes.” *IEEE Transactions on electron devices*, volume 57, no. 1:pp. 12–25, 2009
- [16] Minot, E.D., Kelkensberg, F., Van Kouwen, M., Van Dam, J.A., Kouwenhoven, L.P., Zwiller, V., Borgström, M.T., Wunnicke, O., Verheijen, M.A. and Bakkers, E.P. “Single quantum dot nanowire leds.” *Nano letters*, volume 7, no. 2:pp. 367–371, 2007
- [17] Jing, P., Ji, W., Zeng, Q., Li, D., Qu, S., Wang, J. and Zhang, D. “Vacuum-free transparent quantum dot light-emitting diodes with silver nanowire cathode.” *Scientific reports*, volume 5, no. 1:p. 12499, 2015
- [18] Maslov, A. and Ning, C. “Reflection of guided modes in a semiconductor nanowire laser.” *Applied physics letters*, volume 83, no. 6:pp. 1237–1239, 2003

- [19] Rashidi, A., Monavarian, M., Aragon, A., Okur, S., Nami, M., Rishinaraman-galam, A., Mishkat-Ul-Masabih, S. and Feezell, D. “High-speed nonpolar ingan/-gan leds for visible-light communication.” *IEEE Photonics Technology Letters*, volume 29, no. 4:pp. 381–384, 2017
- [20] Hahn, C., Zhang, Z., Fu, A., Wu, C.H., Hwang, Y.J., Gargas, D.J. and Yang, P. “Epitaxial growth of ingan nanowire arrays for light emitting diodes.” *ACS nano*, volume 5, no. 5:pp. 3970–3976, 2011
- [21] Guo, W., Zhang, M., Banerjee, A. and Bhattacharya, P. “Catalyst-free ingan/-gan nanowire light emitting diodes grown on (001) silicon by molecular beam epitaxy.” *Nano letters*, volume 10, no. 9:pp. 3355–3359, 2010
- [22] Wang, R., Nguyen, H.P., Connie, A.T., Lee, J., Shih, I. and Mi, Z. “Color-tunable, phosphor-free ingan nanowire light-emitting diode arrays monolithically integrated on silicon.” *Optics express*, volume 22, no. 107:pp. A1768–A1775, 2014
- [23] Park, Y., Jahangir, S., Park, Y., Bhattacharya, P. and Heo, J. “Ingan/gan nanowires grown on sio₂ and light emitting diodes with low turn on voltages.” *Optics express*, volume 23, no. 11:pp. A650–A656, 2015
- [24] Ryu, H.Y. and Shim, J.I. “Structural parameter dependence of light extraction efficiency in photonic crystal ingan vertical light-emitting diode structures.” *IEEE Journal of Quantum Electronics*, volume 46, no. 5:pp. 714–720, 2010
- [25] Zhu, P., Liu, G., Zhang, J. and Tansu, N. “FDTD analysis on extraction efficiency of gan light-emitting diodes with microsphere arrays.” *Journal of Display Technology*, volume 9, no. 5:pp. 317–323, 2013
- [26] Huang, C., Zhang, H. and Sun, H. “Ultraviolet optoelectronic devices based on algan-sic platform: Towards monolithic photonics integration system.” *Nano energy*, volume 77:p. 105149, 2020
- [27] Hirayama, H., Fujikawa, S. and Kamata, N. “Recent progress in algan-based deep-uv leds.” *Electronics and Communications in Japan*, volume 98, no. 5:pp. 1–8, 2015
- [28] Hasan, S.M., You, W., Sumon, M.S.I. and Arafin, S. “Recent progress of electrically pumped algan diode lasers in the uv-b and-c bands.” In “Photonics,” volume 8, p. 267. MDPI, 2021

- [29] Zhao, S., Lu, J., Hai, X. and Yin, X. “Algan nanowires for ultraviolet light-emitting: recent progress, challenges, and prospects.” *Micromachines*, volume 11, no. 2:p. 125, 2020
- [30] Moustakas, T.D. and Paiella, R. “Optoelectronic device physics and technology of nitride semiconductors from the uv to the terahertz.” *Reports on Progress in Physics*, volume 80, no. 10:p. 106501, 2017
- [31] Zhao, S. and Mi, Z. “Al (ga) n nanowire deep ultraviolet optoelectronics.” In “Semiconductors and Semimetals,” volume 96, pp. 167–199. Elsevier, 2017
- [32] Sekiguchi, H., Kato, K., Tanaka, J., Kikuchi, A. and Kishino, K. “Ultraviolet gan-based nanocolumn light-emitting diodes grown on n-(111) si substrates by rf-plasma-assisted molecular beam epitaxy.” *physica status solidi (a)*, volume 205, no. 5:pp. 1067–1069, 2008
- [33] Liu, X., Le, B.H., Woo, S.Y., Zhao, S., Pofelski, A., Botton, G.A. and Mi, Z. “Selective area epitaxy of algan nanowire arrays across nearly the entire compositional range for deep ultraviolet photonics.” *Optics express*, volume 25, no. 24:pp. 30494–30502, 2017
- [34] Hai, X., Rashid, R., Sadaf, S., Mi, Z. and Zhao, S. “Effect of low hole mobility on the efficiency droop of algan nanowire deep ultraviolet light emitting diodes.” *Applied Physics Letters*, volume 114, no. 10:p. 101104, 2019
- [35] Sun, H. and Li, X. “Recent advances on iii-nitride nanowire light emitters on foreign substrates—toward flexible photonics.” *physica status solidi (a)*, volume 216, no. 2:p. 1800420, 2019
- [36] Høiaas, I.M., Liudi Mulyo, A., Vullum, P.E., Kim, D.C., Ahtapodov, L., Fimland, B.O., Kishino, K. and Weman, H. “Gan/algan nanocolumn ultraviolet light-emitting diode using double-layer graphene as substrate and transparent electrode.” *Nano letters*, volume 19, no. 3:pp. 1649–1658, 2019
- [37] Coulon, P.M., Kusch, G., Martin, R.W. and Shields, P.A. “Deep uv emission from highly ordered algan/aln core–shell nanorods.” *ACS applied materials & interfaces*, volume 10, no. 39:pp. 33441–33449, 2018
- [38] Brubaker, M.D., Genter, K.L., Roshko, A., Blanchard, P.T., Spann, B.T., Harvey, T.E. and Bertness, K.A. “Uv leds based on p–i–n core–shell algan/gan nanowire heterostructures grown by n-polar selective area epitaxy.” *Nanotechnology*, volume 30, no. 23:p. 234001, 2019

- [39] Wu, Y., Wang, Y., Sun, K. and Mi, Z. “Molecular beam epitaxy and characterization of algan nanowire ultraviolet light emitting diodes on al coated si (0 0 1) substrate.” *Journal of Crystal Growth*, volume 507:pp. 65–69, 2019
- [40] Du, P., Rao, L., Liu, Y., Cheng, Z. et al. “Enhancing the light extraction efficiency of algan led with nanowire photonic crystal and graphene transparent electrode.” *Superlattices and Microstructures*, volume 133:p. 106216, 2019
- [41] Ryu, H.Y. “Large enhancement of light extraction efficiency in algan-based nanorod ultraviolet light-emitting diode structures.” *Nanoscale research letters*, volume 9:pp. 1–7, 2014
- [42] Ryu, H.Y., Choi, I.G., Choi, H.S. and Shim, J.I. “Investigation of light extraction efficiency in algan deep-ultraviolet light-emitting diodes.” *Applied Physics Express*, volume 6, no. 6:p. 062101, 2013
- [43] Guttman, M., Mehnke, F., Belde, B., Wolf, F., Reich, C., Sulmoni, L., Wernicke, T. and Kneissl, M. “Optical light polarization and light extraction efficiency of algan-based leds emitting between 264 and 220 nm.” *Japanese Journal of Applied Physics*, volume 58, no. SC:p. SCCB20, 2019
- [44] Kolbe, T., Knauer, A., Chua, C., Yang, Z., Einfeldt, S., Vogt, P., Johnson, N.M., Weyers, M. and Kneissl, M. “Optical polarization characteristics of ultraviolet (in)al gan multiple quantum well light emitting diodes.” *Applied Physics Letters*, volume 97, no. 17:p. 171105, 2010
- [45] Shakya, J., Knabe, K., Kim, K., Li, J., Lin, J. and Jiang, H. “Polarization of iii-nitride blue and ultraviolet light-emitting diodes.” *Applied Physics Letters*, volume 86, no. 9:p. 091107, 2005
- [46] Reich, C., Guttman, M., Feneberg, M., Wernicke, T., Mehnke, F., Kuhn, C., Rass, J., Lapeyrade, M., Einfeldt, S., Knauer, A. et al. “Strongly transverse-electric-polarized emission from deep ultraviolet algan quantum well light emitting diodes.” *Applied Physics Letters*, volume 107, no. 14:p. 142101, 2015
- [47] Jia, C., Yu, T., Mu, S., Pan, Y., Yang, Z., Chen, Z., Qin, Z. and Zhang, G. “Polarization of edge emission from iii-nitride light emitting diodes of emission wavelength from 395 to 455 nm.” *Applied physics letters*, volume 90, no. 21:p. 211112, 2007
- [48] Zhao, L.X., Yu, Z.G., Sun, B., Zhu, S.C., An, P.B., Yang, C., Liu, L., Wang, J.X. and Li, J.M. “Progress and prospects of gan-based leds using nanostructures.” *Chinese Physics B*, volume 24, no. 6:p. 068506, 2015

- [49] Nakamura, S. and Krames, M.R. “History of gallium–nitride-based light-emitting diodes for illumination.” *Proceedings of the IEEE*, volume 101, no. 10:pp. 2211–2220, 2013
- [50] Cho, H.K., Jang, J., Choi, J.H., Choi, J., Kim, J., Lee, J.S., Lee, B., Choe, Y.H., Lee, K.D., Kim, S.H. et al. “Light extraction enhancement from nanoimprinted photonic crystal gan-based blue light-emitting diodes.” *Optics Express*, volume 14, no. 19:pp. 8654–8660, 2006
- [51] Shatalov, M., Sun, W., Lunev, A., Hu, X., Dobrinsky, A., Bilenko, Y., Yang, J., Shur, M., Gaska, R., Moe, C. et al. “Algan deep-ultraviolet light-emitting diodes with external quantum efficiency above 10%.” *Applied Physics Express*, volume 5, no. 8:p. 082101, 2012
- [52] Cao, Y., Wang, N., Tian, H., Guo, J., Wei, Y., Chen, H., Miao, Y., Zou, W., Pan, K., He, Y. et al. “Perovskite light-emitting diodes based on spontaneously formed submicrometre-scale structures.” *Nature*, volume 562, no. 7726:pp. 249–253, 2018
- [53] Liu, Z., Liu, S., Wang, K. and Luo, X. “Analysis of factors affecting color distribution of white leds.” In “2008 International conference on electronic packaging technology & high density packaging,” pp. 1–8. IEEE, 2008
- [54] Shatalov, M., Jain, R., Dobrinsky, A., Sun, W., Bilenko, Y., Yang, J., Shur, M. and Gaska, R. “High-efficiency uv leds on sapphire.” In “Gallium Nitride Materials and Devices X,” volume 9363, pp. 203–209. SPIE, 2015
- [55] Windisch, R., Dutta, B., Kuijk, M., Knobloch, A., Meinschmidt, S., Schoberth, S., Kiesel, P., Borghe, G., Dohler, G.H. and Heremans, P. “40% efficient thin-film surface-textured light-emitting diodes by optimization of natural lithography.” *IEEE Transactions on Electron Devices*, volume 47, no. 7:pp. 1492–1498, 2000
- [56] Luo, W., Sadaf, S.M., Ahmed, T., Baten, M.Z., Faruque, M.O., Hossain, M.A., Wang, H., Li, Y., Yuan, Y., Wang, W. et al. “Breaking the transverse magnetic-polarized light extraction bottleneck of ultraviolet-c light-emitting diodes using nanopatterned substrates and an inclined reflector.” *ACS Photonics*, volume 9, no. 9:pp. 3172–3179, 2022
- [57] Ra, Y.H. and Lee, C.R. “Monolithic light reflector-nanowire light emitting diodes.” *Advanced Materials Technologies*, volume 6, no. 2:p. 2000885, 2021
- [58] Lin, J. and Jiang, H. “Development of microled.” *Applied Physics Letters*, volume 116, no. 10:p. 100502, 2020

- [59] Anwar, A.R., Sajjad, M.T., Johar, M.A., Hernández-Gutiérrez, C.A., Usman, M. and Łepkowski, S. “Recent progress in micro-led-based display technologies.” *Laser & Photonics Reviews*, volume 16, no. 6:p. 2100427, 2022
- [60] Huang, Y., Hsiang, E.L., Deng, M.Y. and Wu, S.T. “Mini-led, micro-led and oled displays: present status and future perspectives.” *Light: Science & Applications*, volume 9, no. 1:p. 105, 2020
- [61] Wu, Y., Ma, J., Su, P., Zhang, L. and Xia, B. “Full-color realization of micro-led displays.” *Nanomaterials*, volume 10, no. 12:p. 2482, 2020
- [62] Ohta, Y., Guinto, M.C., Tokuda, T., Kawahara, M., Haruta, M., Takehara, H., Tashiro, H., Sasagawa, K., Onoe, H., Yamaguchi, R. et al. “Micro-led array-based photo-stimulation devices for optogenetics in rat and macaque monkey brains.” *IEEE Access*, volume 9:pp. 127937–127949, 2021
- [63] Lee, K., Cho, I., Kang, M., Jeong, J., Choi, M., Woo, K.Y., Yoon, K.J., Cho, Y.H. and Park, I. “Ultra-low-power e-nose system based on multi-micro-led-integrated, nanostructured gas sensors and deep learning.” *ACS nano*, 2022
- [64] Hayden, O., Agarwal, R. and Lu, W. “Semiconductor nanowire devices.” *Nano Today*, volume 3, no. 5-6:pp. 12–22, 2008
- [65] Pan, C., Dong, L., Zhu, G., Niu, S., Yu, R., Yang, Q., Liu, Y. and Wang, Z.L. “High-resolution electroluminescent imaging of pressure distribution using a piezoelectric nanowire led array.” *Nature Photonics*, volume 7, no. 9:pp. 752–758, 2013
- [66] Laubsch, A., Sabathil, M., Baur, J., Peter, M. and Hahn, B. “High-power and high-efficiency ingan-based light emitters.” *IEEE transactions on electron devices*, volume 57, no. 1:pp. 79–87, 2009
- [67] Li, D., Jiang, K., Sun, X. and Guo, C. “Algan photonics: recent advances in materials and ultraviolet devices.” *Advances in Optics and Photonics*, volume 10, no. 1:pp. 43–110, 2018
- [68] Henneghien, A.L., Tourbot, G., Daudin, B., Lartigue, O., Desieres, Y. and Gérard, J.M. “Optical anisotropy and light extraction efficiency of mbe grown gan nanowires epilayers.” *Optics Express*, volume 19, no. 2:pp. 527–539, 2011
- [69] Johar, M.A., Song, H.G., Waseem, A., Hassan, M.A., Bagal, I.V., Cho, Y.H. and Ryu, S.W. “Universal and scalable route to fabricate gan nanowire-based led on

- amorphous substrate by mocvd.” *Applied Materials Today*, volume 19:p. 100541, 2020
- [70] Bulashevich, K.A., Konoplev, S.S. and Karpov, S.Y. “Effect of die shape and size on performance of iii-nitride micro-leds: A modeling study.” In “Photonics,” volume 5, p. 41. MDPI, 2018
- [71] Li, X.H., Song, R., Ee, Y.K., Kumnorkaew, P., Gilchrist, J.F. and Tansu, N. “Light extraction efficiency and radiation patterns of iii-nitride light-emitting diodes with colloidal microlens arrays with various aspect ratios.” *IEEE Photonics Journal*, volume 3, no. 3:pp. 489–499, 2011
- [72] Wiesmann, C., Bergenek, K., Linder, N. and Schwarz, U.T. “Photonic crystal leds—designing light extraction.” *Laser & Photonics Reviews*, volume 3, no. 3:pp. 262–286, 2009
- [73] Jeon, S., Lee, S., Han, K.H., Shin, H., Kim, K.H., Jeong, J.H. and Kim, J.J. “High-quality white oleds with comparable efficiencies to leds.” *Advanced Optical Materials*, volume 6, no. 8:p. 1701349, 2018
- [74] Tsai, Y.L., Lai, K.Y., Lee, M.J., Liao, Y.K., Ooi, B.S., Kuo, H.C. and He, J.H. “Photon management of gan-based optoelectronic devices via nanoscaled phenomena.” *Progress in Quantum Electronics*, volume 49:pp. 1–25, 2016
- [75] Zhang, Q., Li, K. and Choi, H. “Ingan light-emitting diodes with indium-tin-oxide sub-micron lenses patterned by nanosphere lithography.” *Applied Physics Letters*, volume 100, no. 6, 2012
- [76] Huang, H.W., Kao, C., Chu, J., Kuo, H.C., Wang, S. and Yu, C. “Improvement of ingan-gan light-emitting diode performance with a nano-roughened p-gan surface.” *IEEE Photonics Technology Letters*, volume 17, no. 5:pp. 983–985, 2005
- [77] Matioli, E. and Weisbuch, C. “Impact of photonic crystals on led light extraction efficiency: approaches and limits to vertical structure designs.” *Journal of Physics D: Applied Physics*, volume 43, no. 35:p. 354005, 2010
- [78] Zhang, Z., Gao, F. and Li, G. “Theoretically enhance the vertical light extraction efficiency of the algan-based nanowire photonic crystal ultraviolet light-emitting diodes by selecting the band gap.” *IEEE Photonics Journal*, volume 13, no. 3:pp. 1–11, 2021

- [79] Chen, J., Wang, T. and Wang, X. “Enhancing light extraction efficiency of gan led by combining complex-period photonic crystals with doping.” *Journal of the American Ceramic Society*, 2023
- [80] Ee, Y.K., Arif, R.A., Tansu, N., Kumnorkaew, P. and Gilchrist, J.F. “Enhancement of light extraction efficiency of ingan quantum wells light emitting diodes using sio₂/polystyrene microlens arrays.” *Applied Physics Letters*, volume 91, no. 22, 2007
- [81] Song, Y.M., Choi, E.S., Park, G.C., Park, C.Y., Jang, S.J. and Lee, Y.T. “Disordered antireflective nanostructures on gan-based light-emitting diodes using ag nanoparticles for improved light extraction efficiency.” *Applied Physics Letters*, volume 97, no. 9, 2010
- [82] Hsiao, Y.H., Chen, C.Y., Huang, L.C., Lin, G.J., Lien, D.H., Huang, J.J. and He, J.H. “Light extraction enhancement with radiation pattern shaping of leds by waveguiding nanorods with impedance-matching tips.” *Nanoscale*, volume 6, no. 5:pp. 2624–2628, 2014
- [83] Kao, C.C., Su, Y.K., Lin, C.L. and Chen, J.J. “The aspect ratio effects on the performances of gan-based light-emitting diodes with nanopatterned sapphire substrates.” *Applied Physics Letters*, volume 97, no. 2, 2010
- [84] Li, Y., You, S., Zhu, M., Zhao, L., Hou, W., Detchprohm, T., Taniguchi, Y. and Tamura, N. “S, tanaka, and c. wetzel.” *Appl. Phys. Lett*, volume 98, no. 15:p. 151102, 2011
- [85] Yee, K.S. and Chen, J.S. “The finite-difference time-domain (fdtd) and the finite-volume time-domain (fvtd) methods in solving maxwell’s equations.” *IEEE Transactions on Antennas and Propagation*, volume 45, no. 3:pp. 354–363, 1997
- [86] FDominec,. “File:fdtd yee grid 2d-3d.svg.” https://commons.wikimedia.org/wiki/File:FDTD_Yee_grid_2d-3d.svg, January 2015
- [87] Memon, N., Naich, M.R., Pathan, A.Z., Mirjat, B.A. and Faiz, M. “Computational investigations on czts thin-film layers adopting grating structures.” *SSRG International Journal of Electronics and Communication Engineering*, volume 6, no. 8:pp. 38–43, 2019
- [88] Henneghien, A.L., Gayral, B., Désières, Y. and Gérard, J.M. “Simulation of waveguiding and emitting properties of semiconductor nanowires with hexagonal or circular sections.” *JOSA B*, volume 26, no. 12:pp. 2396–2403, 2009

- [89] Ding, K., Avrutin, V., Özgür, Ü. and Morkoç, H. “Status of growth of group iii-nitride heterostructures for deep ultraviolet light-emitting diodes.” *Crystals*, volume 7, no. 10:p. 300, 2017
- [90] Northrup, J., Chua, C., Yang, Z., Wunderer, T., Kneissl, M., Johnson, N. and Kolbe, T. “Effect of strain and barrier composition on the polarization of light emission from algan/aln quantum wells.” *Applied Physics Letters*, volume 100, no. 2:p. 021101, 2012